AGA 414: Métodos Observacionais

Jorge Meléndez

Fotometria I

Introdução, sistemas fotométricos, aplicações,

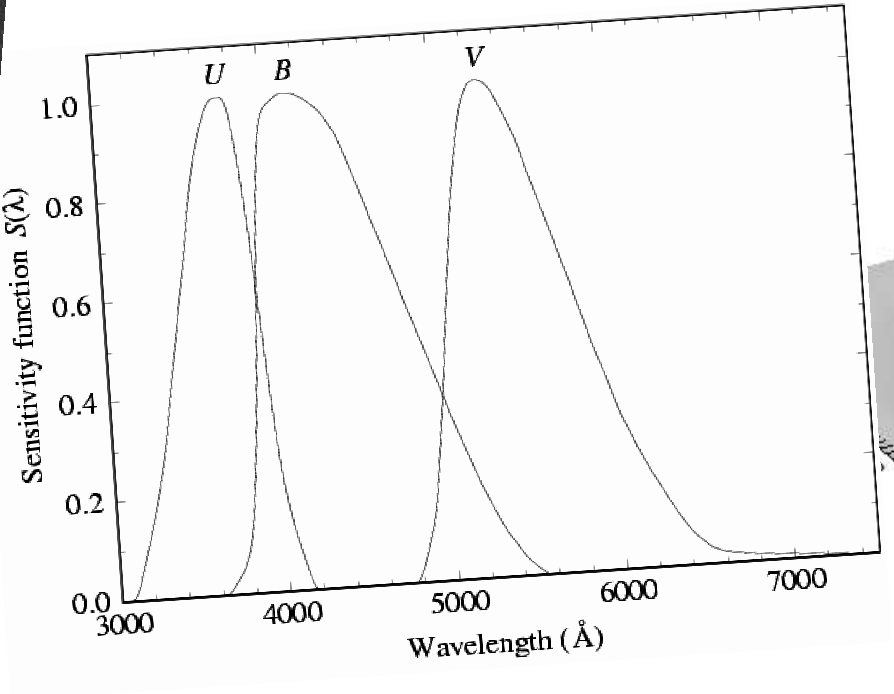

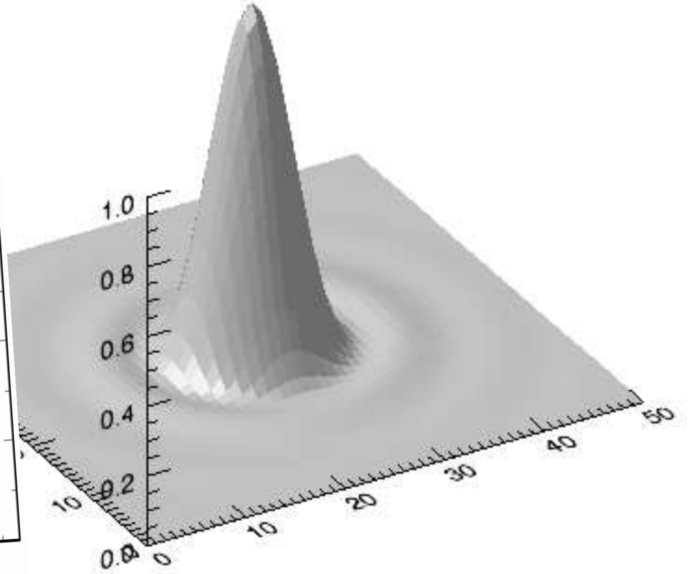

Atualização: 02/04/2014

Fotometria: fluxo (ou intensidade) em uma banda larga (ou intermediaria) do espectro

Espectroscopia: medidas do fluxo relativo, a baixa, media ou alta resolução espectral

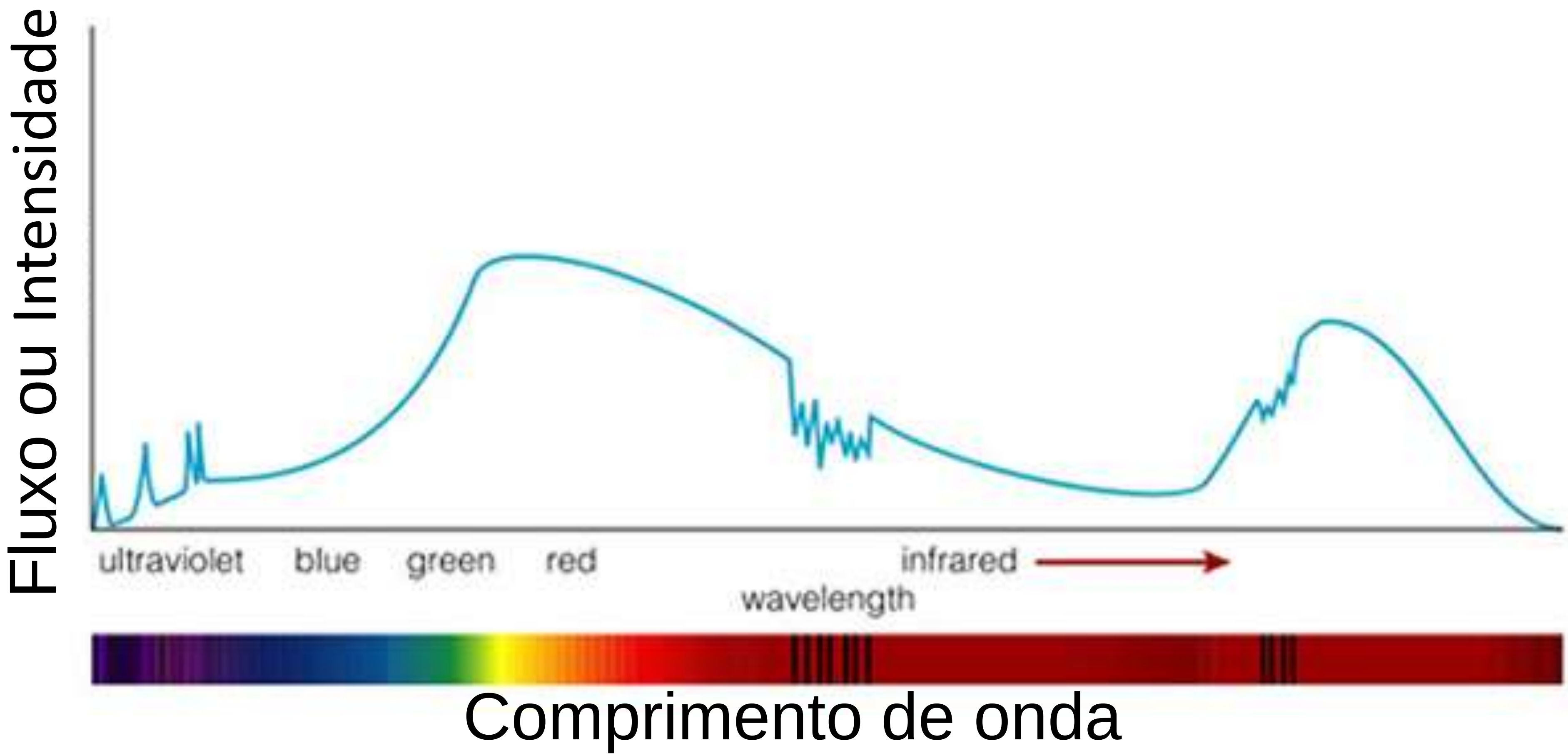

Espectrofotometria: Distribuicao do Fluxo (ou intensidade) em baixa resolução espectral

Espectrofotometria da estrela 56 Ari

(observações de Adelman no ótico e espectro IUE no UV)

A&A 509, A28 (2010)

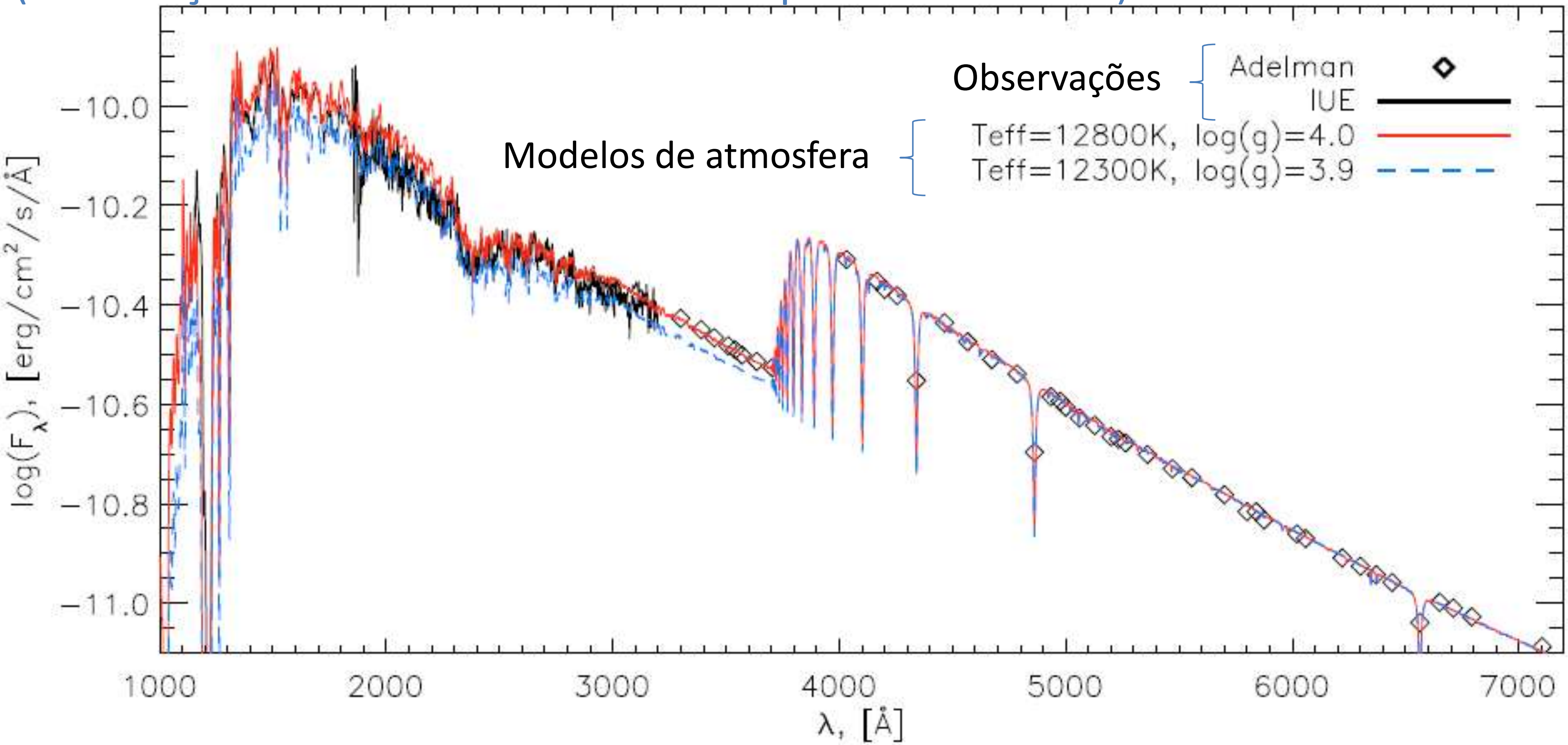

Fig. 1. Comparison of the observed and computed spectral energy distributions of 56 Ari. Theoretical models correspond to T_{eff} = 12 300 K, log(g) = 3.9 and T_{eff} = 12 800 K, log(g) = 4.0. The model fluxes have been convolved with an $FWHM$ = 10 Å Gaussian kernel for a better view.

D. Shulyak[1], O. Kochukhov[2], G. Valyavin[3], B.-C. Lee[4], G. Galazutdinov[5], K.-M. Kim[4], I. Han[4], and T. Burlakova[6]

Fotometria relativa (ou diferencial)

- Por exemplo, medir a brilho da estrela A em relação à estrela P, sem conhecer (necessariament) a magnitude da estrela P

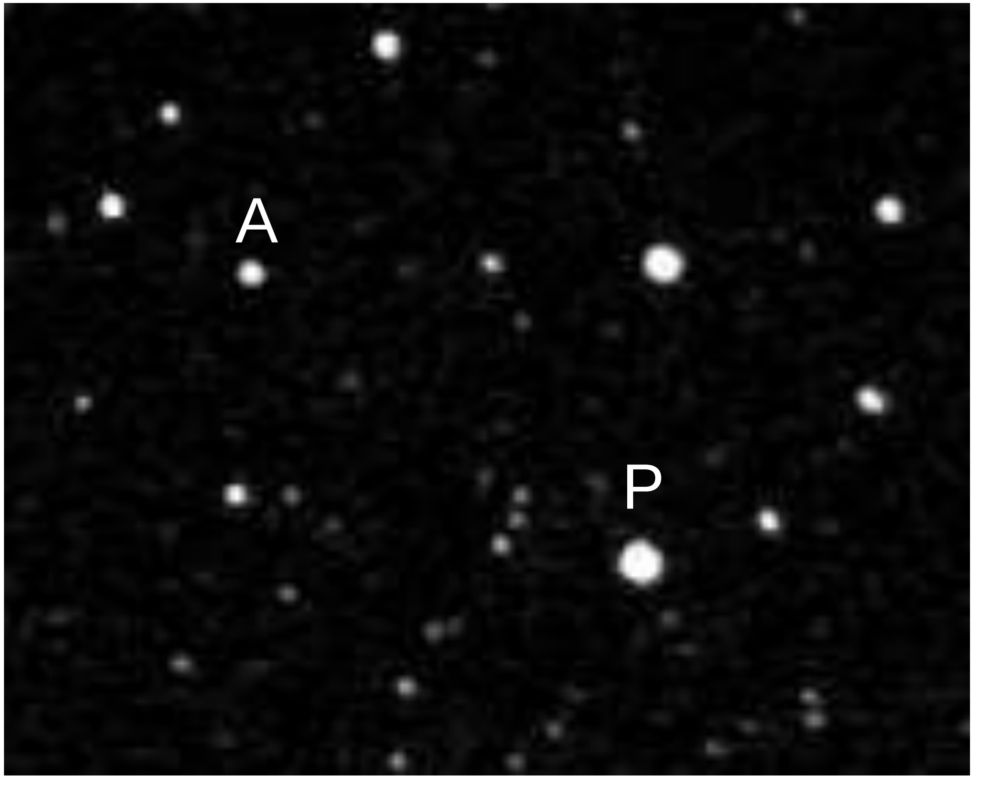

Fotometria relativa (ou diferencial)

- Periodo de rotação de um asteroide

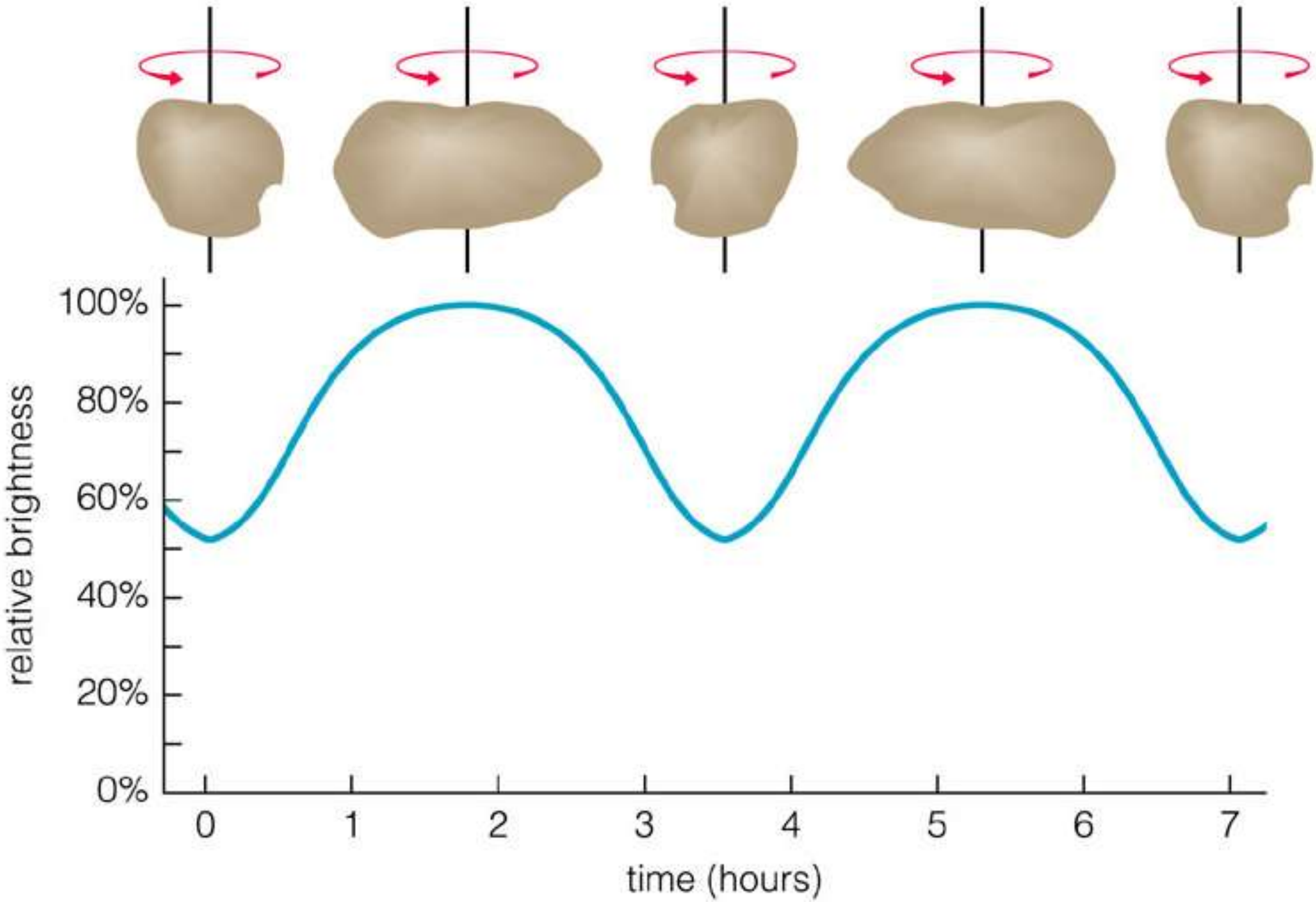

Fotometria absoluta

- Medida do brilho de objetos em um sistema padrão
- É possível comparar com outros observadores
- Podemos transformar magnitudes em fluxos absolutos

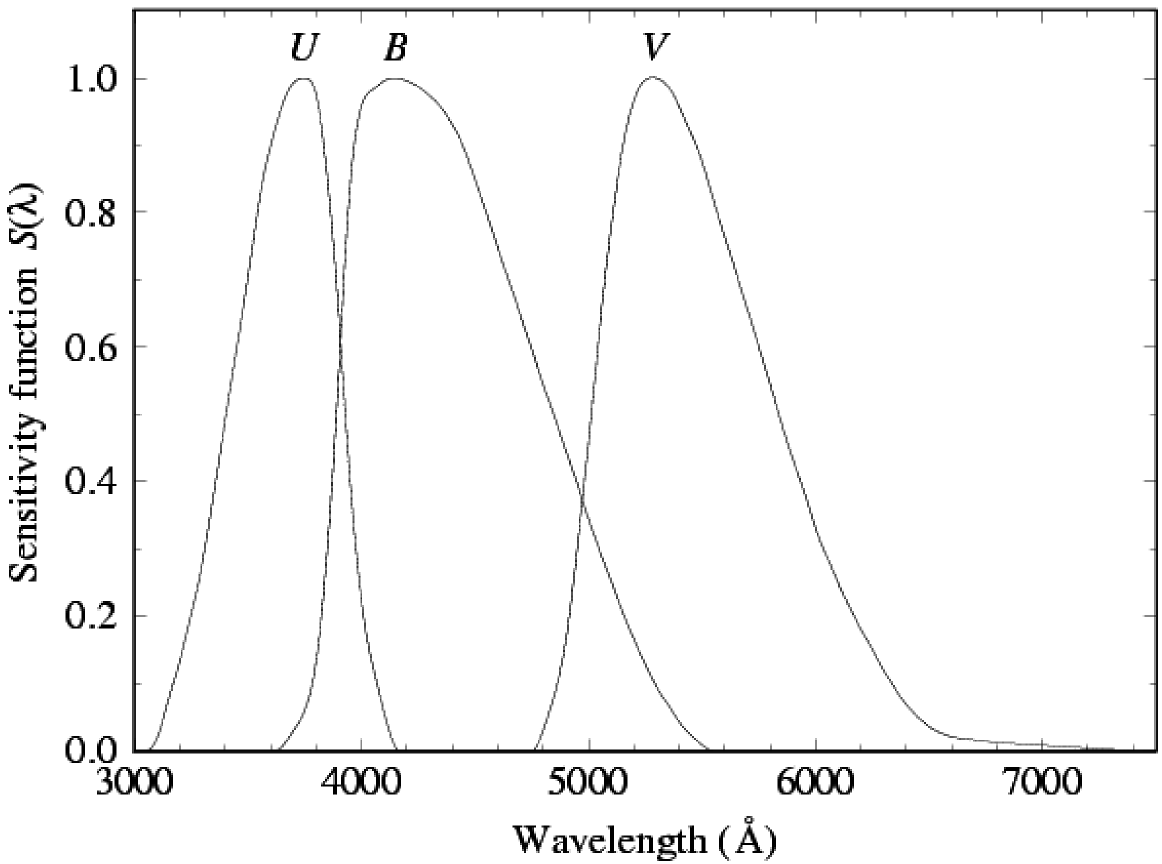

Historicamente …

Hiparcos (190-125 a.C)

- Baseado no brilho aparente a olho nu
- Mais brilhantes: classe 1
- Mais fracas: classe 6

Magnitudes

estrelas mais brilhantes a olho nú: *m* ~ -1 a 0

mais fracas: *m* ~ 5 a 6

Escala logarítmica

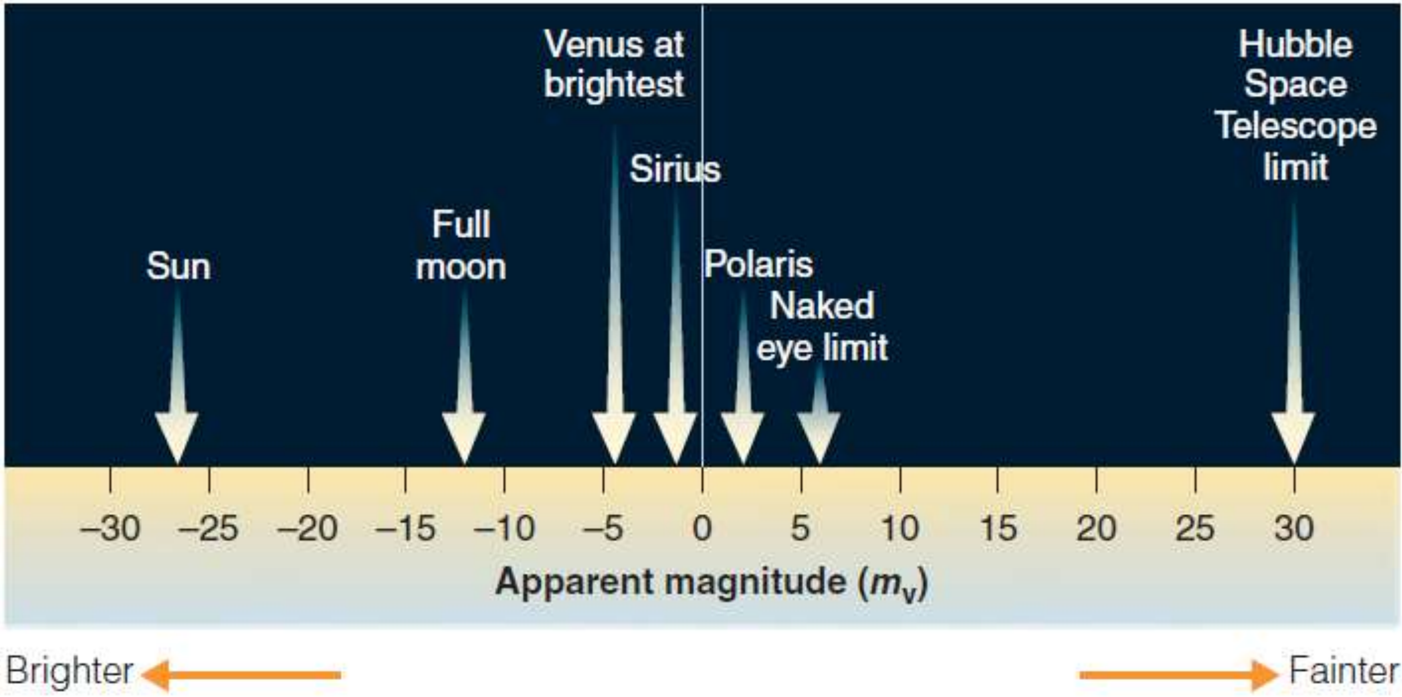

Pogson (1856): escala logarítmica

Magnitude (m) e fluxo (f):

$\Delta m = 5 \rightarrow f_1/f_2 = 100$

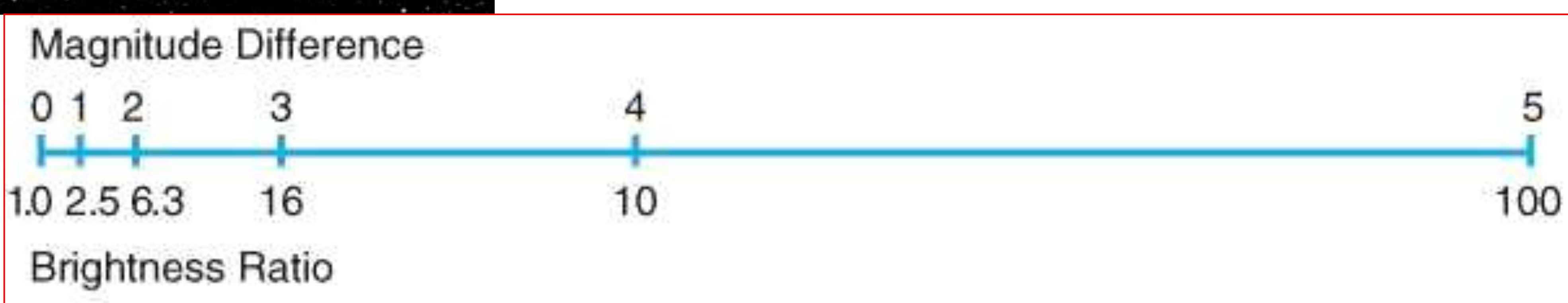

Relações entre
magnitude aparente m e *fluxo f*

$$m_1 - m_2 = -2.5 \log(f_1/f_2)$$

$$f_1/f_2 = 10^{-0.4(m_1 - m_2)}$$

Exemplo, uma Δ = -1 mag equivale a uma razão de fluxo de ...

$$f_1/f_2 = 10^{-0.4*-1} = 10^{+0.4} = 2.512$$

Exemplo: quão mais brilhante é a estrela *Vega* (m ~ 0) em relação a *18 Sco* (m ~ 5)

m_1 (Vega) = 0,0

m_2 (18 Sco) = 5,0

$m_1 - m_2 = -2,5 \log(f_1/f_2)$

$$-5,0 = -2,5 \log (f_1/f_2)$$

$$2,0 = \log (f_1/f_2)$$

$f_1/f_2 = 10^2 = 100$

Vega é 100 vezes mais brilhante que 18 Sco

Exemplo: tempo de exposição

Se uma estrela de m = x precisa de um tempo de 11 seg, qual será o tempo para uma estrela de m = x + 2?

$$f_1/f_2 = 10^{-0.4(m_1 - m_2)}$$

$$f_2/f_1 = 10^{+0.4(m_1 - m_2)} = 2.51^{(m_1 - m_2)}$$

$m_1 = x$, $m_2 = x + 2$, então $m_1 - m_2 = -2$

$$f_2/f_1 = 2.512^{-2} = 0.16$$

Fluxo 0.16 veces menor, então precisa de tempo de exposição 11/0.16 veces maior = 69s

Tempo de exposição

Menor fluxo precisa de mais tempo de exposição, portanto podemos escrever a relação entre tempo e magnitudes:

$$f_1/f_2 = 10^{-0.4(m_1 - m_2)}$$

$$t_2/t_1 = 10^{-0.4(m_1 - m_2)}$$

$$t_2/t_1 = 10^{+0.4(m_2 - m_1)} = 2.51^{(m_2 - m_1)}$$

$$\mathbf{t_2/t_1 = 2.512^{(m_2 - m_1)}}$$

Conhecendo o tempo t_1 para um objeto m_1 (por exemplo pela calculadora de tempo do instrumento) podemos determinar os outros tempos de exposição.

Distância

$$d = 1/\, p('')$$

p : parallaxe em segundos de arco

d: distância em unidades de parsecs

1 parsec = $3{,}0857 \times 10^{16}$ metros

= 3,2616 anos-luz

Exemplo:

p = 0,5”

d = 2 parsec = 6,5 anos-luz

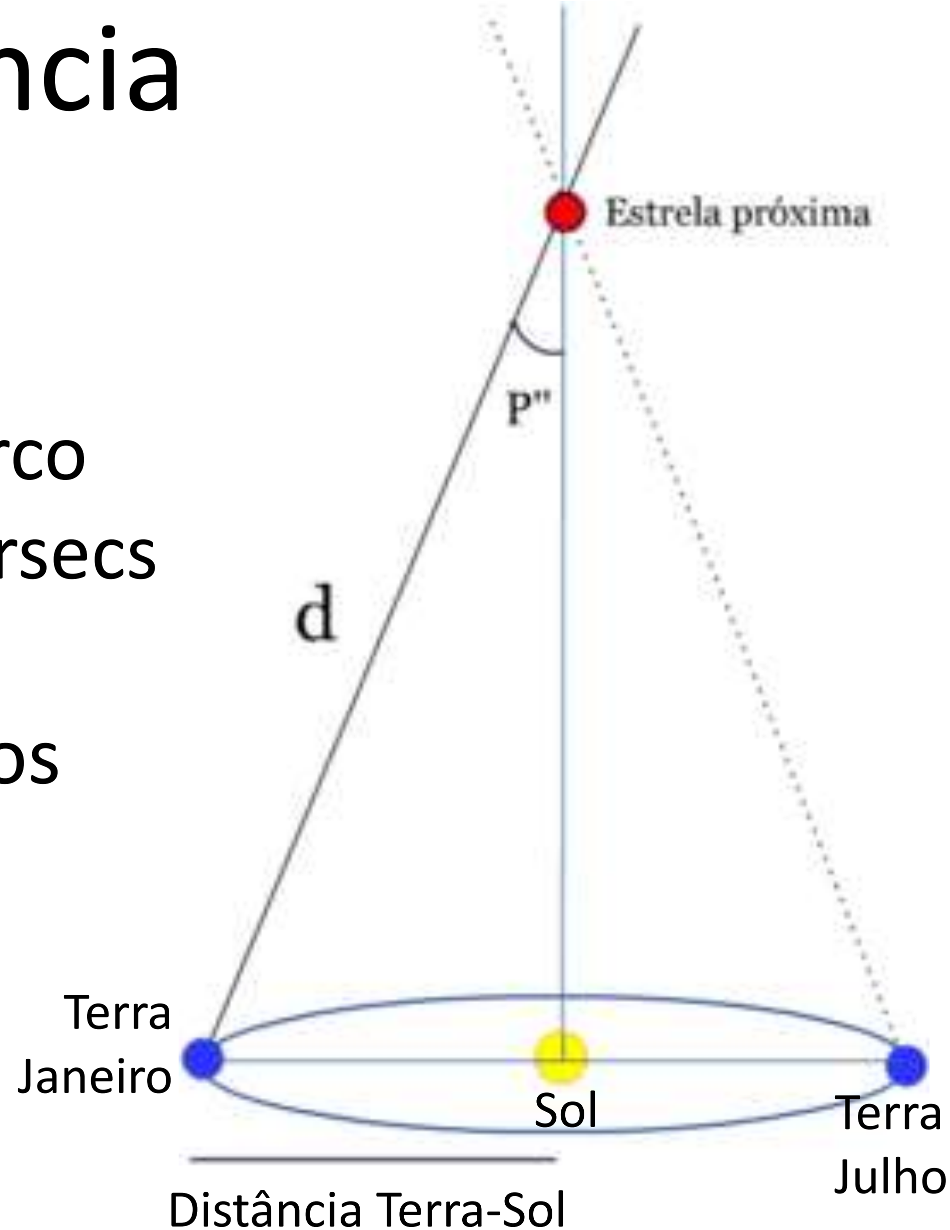

Magnitude absoluta: M

A *magnitude aparente* m não oferece informação sobre o *brilho* ***intrínseco*** da estrela

Magnitude absoluta M: a magnitude aparente que teria um objeto a 10pc de distância

$$m - M = 5 \log d - 5$$

$$M = m + 5 \log p + 5$$

d : parsecs
p : ” (arcsec)

Exemplo: Magnitude Absoluta de gêmea solar *18 Sco*

http://simbad.u-strasbg.fr/simbad/sim-fid

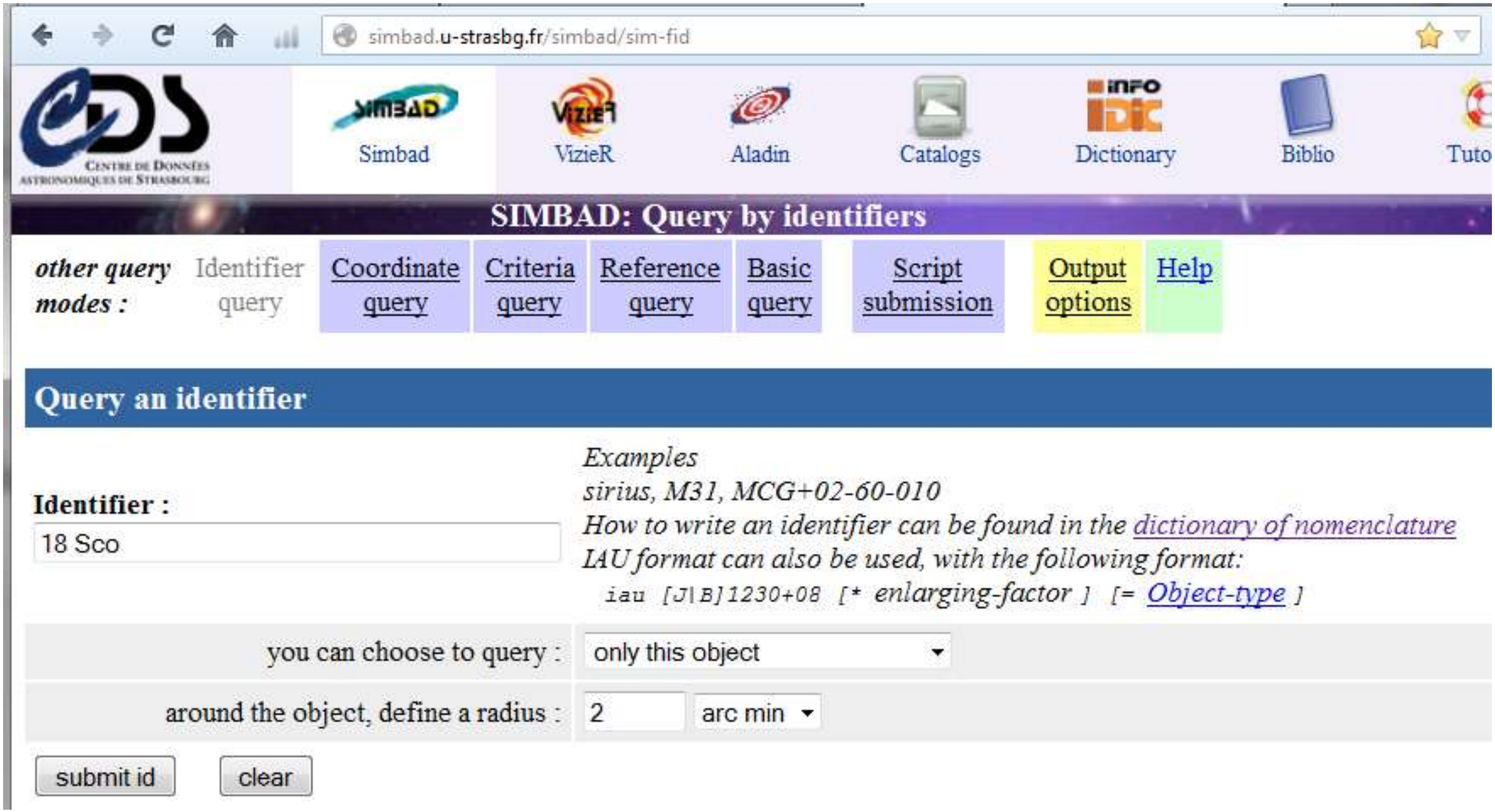

simbad.u-strasbg.fr/simbad/sim-id?Ident=18+Sco&NbIdent=1&Radius=2&Radius.unit=arcmin&submit=submit+ic

Basic data :

*** 18 Sco -- Variable Star**

query around with radius

Other object types:	* (*,BD,CSI,GC,GCRV,GEN#,GJ,HD,HIC,HIP,HR,L [B10]) , **PM*** (Ci,LFT,LHS,LTT,NLTT,PM) , ** (TD1)
ICRS coord. (ep=J2000) :	**16 15 37.26946 -08 22 09.9870 (Optical)**
FK5 coord. (ep=J2000 eq=2000) :	**16 15 37.269 -08 22 09.99 (Optical) [4**
FK4 coord. (ep=B1950 eq=1950) :	**16 12 53.98 -08 14 19.0 (Optical) [25.**
Gal coord. (ep=J2000) :	**004.6952 +29.1570 (Optical) [4.48 2.90**
Proper motions *mas/yr* [error ellipse]:	**230.77 -495.53 [0.51 0.33 0] A 2007A&A...**
Radial velocity / Redshift / cz :	**V(km/s) 10.6 [2] / z(~) 0.000035 [0.00000**
Parallaxes *mas*:	**71.94 [0.37] A 2007A&A...474..653V**
Spectral type:	**G2Va C 2011ARep...55...31S**
Fluxes (5) :	**B 6.15 [~] C ~**
	V 5.50 [~] C ~

m.a.s. = 10^{-3} ”

Magnitude m_V

$p = 71,94 \times 10^{-3}$ ”

$m_V = 5,5$

Magnitude Absoluta de *18 Sco*

Magnitude absoluta M: a magnitude aparente *m* que teria um objeto a 10 pc de distância

$$M = m + 5 - 5 \log d \quad [d: \text{parsecs}]$$

$$\mathbf{M = m + 5 + 5 \log \boldsymbol{p}} \; [p: \textit{parallax em}\ ”]$$

$$m_V = 5{,}5;\ p = 71{,}94 \times 10^{-3}\ ”$$

$$M_V = 5{,}5 + 5 + 5 \log (71{,}94 \times 10^{-3})$$

$$= 10{,}5 + 5 \times (\mathbf{-1.14})$$

$$= 4{,}8$$

Para comparação, Sol tem $M_V = 4.83$

As estrelas emitem em diferentes cores

$$B_\lambda(T) = \frac{2hc^2}{\lambda^5} \frac{1}{e^{(hc/\lambda kT)} - 1}$$

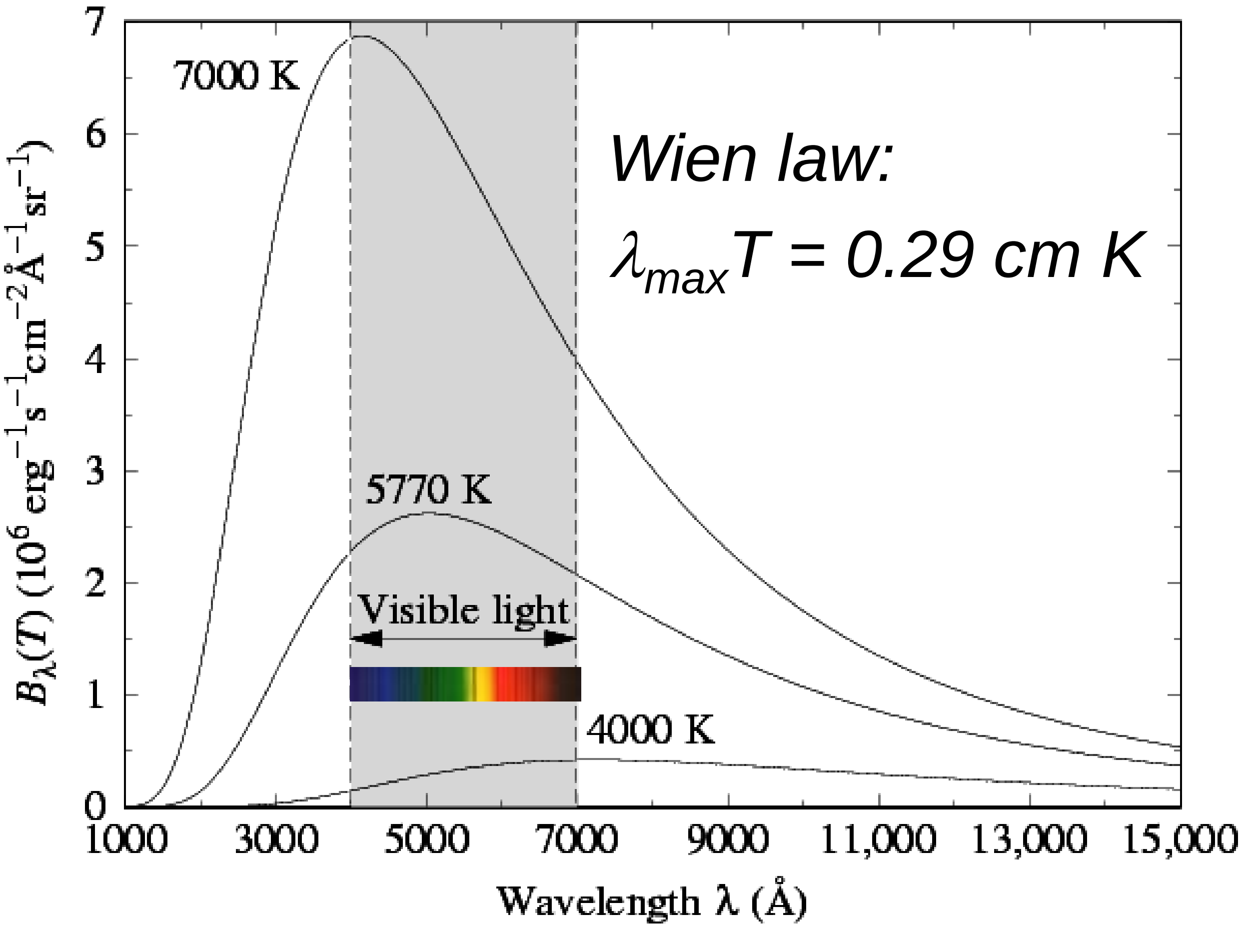

Nosso olho enxerga apenas uma parte da SED

Sistemas fotométricos e aplicações

THE ASTROPHYSICAL JOURNAL, 626:465–485, 2005 June 10

THE EFFECTIVE TEMPERATURE SCALE OF FGK STARS. II. T_{eff} : COLOR : [Fe/H] CALIBRATIONS

IVÁN RAMÍREZ[1]
Department of Astronomy, University of Texas at Austin, RLM 15.306, Austin, TX 78712-1083; ivan@astro.as.utexas.edu
AND
JORGE MELÉNDEZ[1]
Department of Astronomy, California Institute of Technology, MS 105-24, Pasadena, CA 91125; jorge@astro.caltech.edu

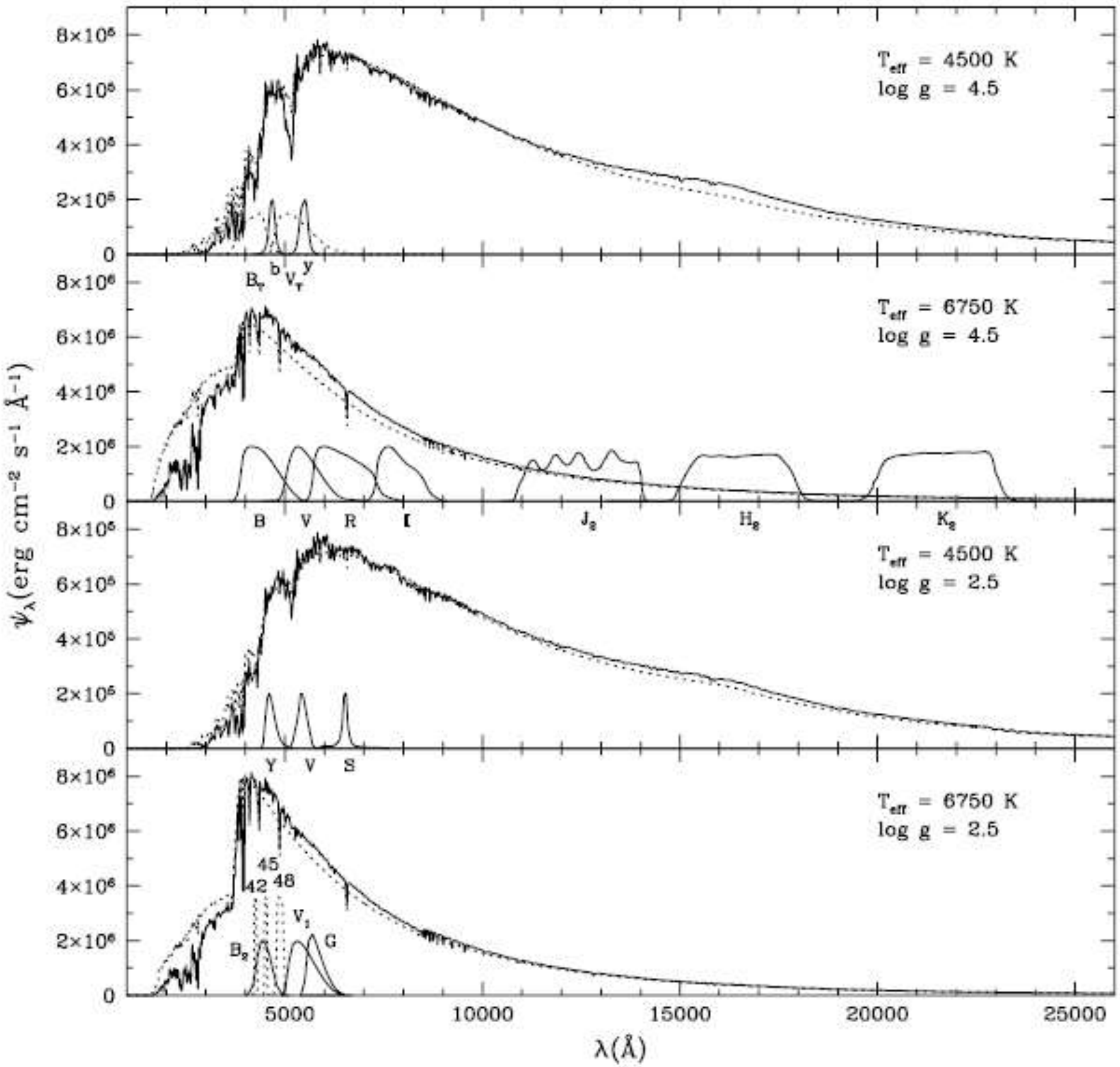

FIG. 7.—Spectral energy distributions from Kurucz models, as given by Lejeune et al. (1997), for atmospheric parameters representative of cool ($T_{eff} = 4500$ K), hot ($T_{eff} = 6750$ K), giant ($\log g = 2.5$), dwarf ($\log g = 4.5$), metal-poor ([Fe/H] $= -2.5$; *dotted lines*), and metal-rich ([Fe/H] $= +0.0$; *solid lines*) stars. The filter transmission functions of interest to this work are also shown.

Na retina há 2 tipos de células responsáveis pelo sentido da visão

Nosso olho definiu o primeiro sistema fotométrico

BASTONETE

CONE

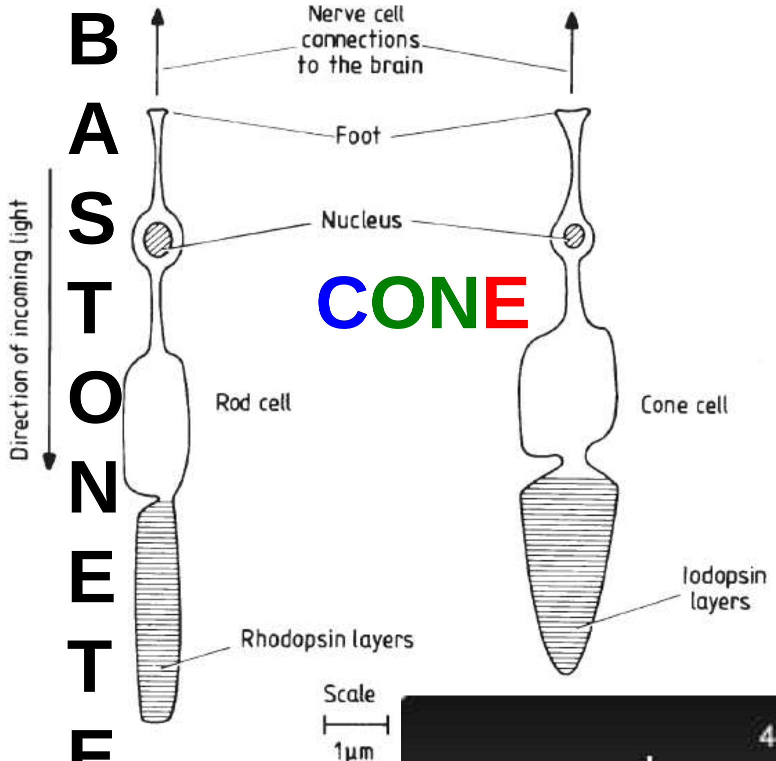

Retinal receptor cells.

Curva de absorção da rodopsina (bastonete)

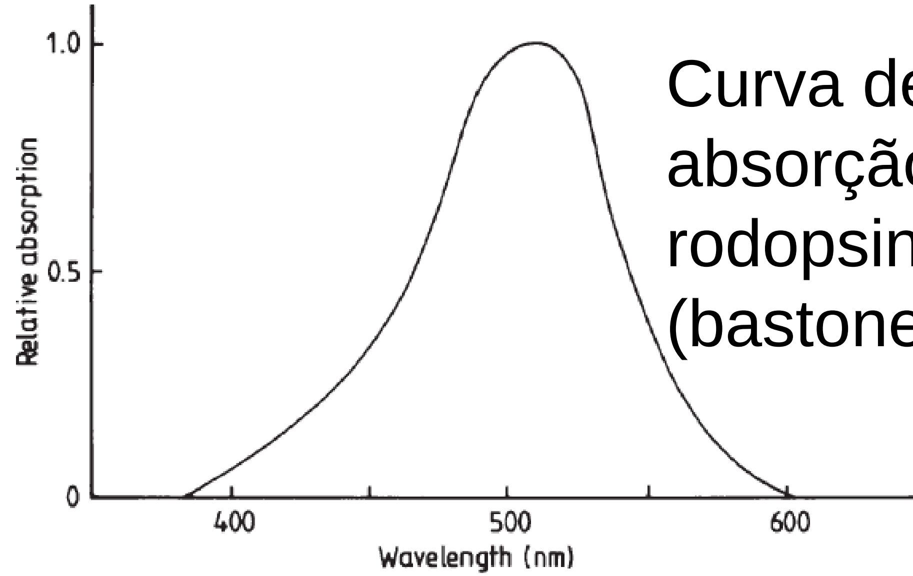

Rhodopsin absorption curve.

$$F = \frac{\int_0^\infty f(\lambda) s(\lambda) d\lambda}{\int_0^\infty s(\lambda) d\lambda}$$

Curvas de absorção dos pigmentos na visão de cone

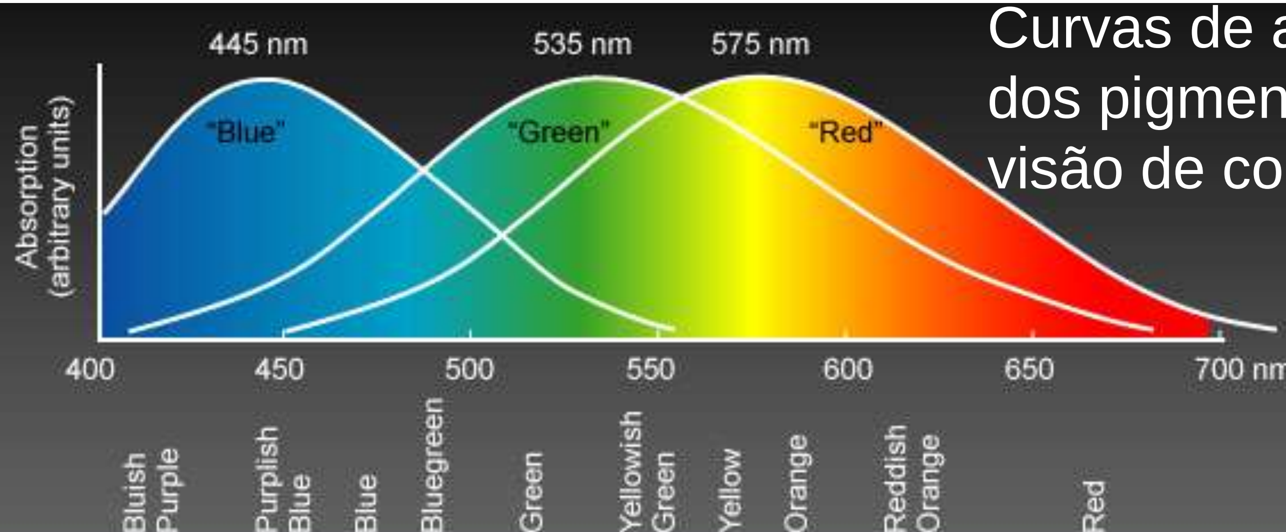

Sistema instrumental

Fluxo observado *F*:

$$F = \frac{\int_0^\infty f(\lambda)s(\lambda)d\lambda}{\int_0^\infty s(\lambda)d\lambda}$$

Sensibilidade *s(λ)* do bastonete

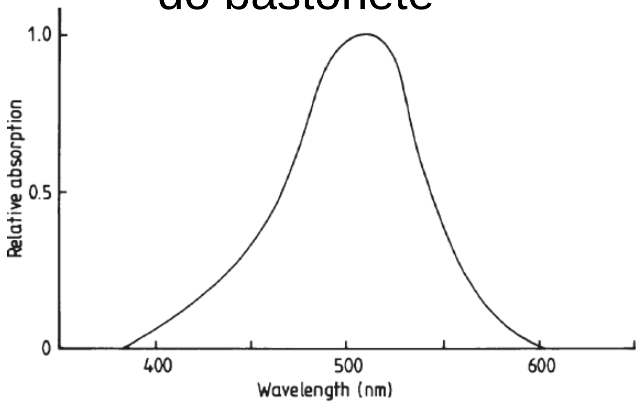

Rhodopsin absorption curve.

- *f(λ)*: fluxo do objeto fora da atmosfera terrestre
- *s(λ)*: função de transmissão (curva de sensibilidade [transmissão do filtro]; detetor; atmosfera; ...)

Existem centenas de sistemas fotométricos ...

Annu. Rev. Astron. Astrophys. 2005. 43:293–336
doi: 10.1146/annurev.astro.41.082801.100251

STANDARD PHOTOMETRIC SYSTEMS

Michael S. Bessell
Research School of Astronomy and Astrophysics, The Australian National University, Weston, ACT 2611, Australia; email: bessell@mso.anu.edu.au

Mike Bessell. *Autoridade mundial em sistemas fotométricos*

Sistemas fotométricos de banda larga: **UBV**

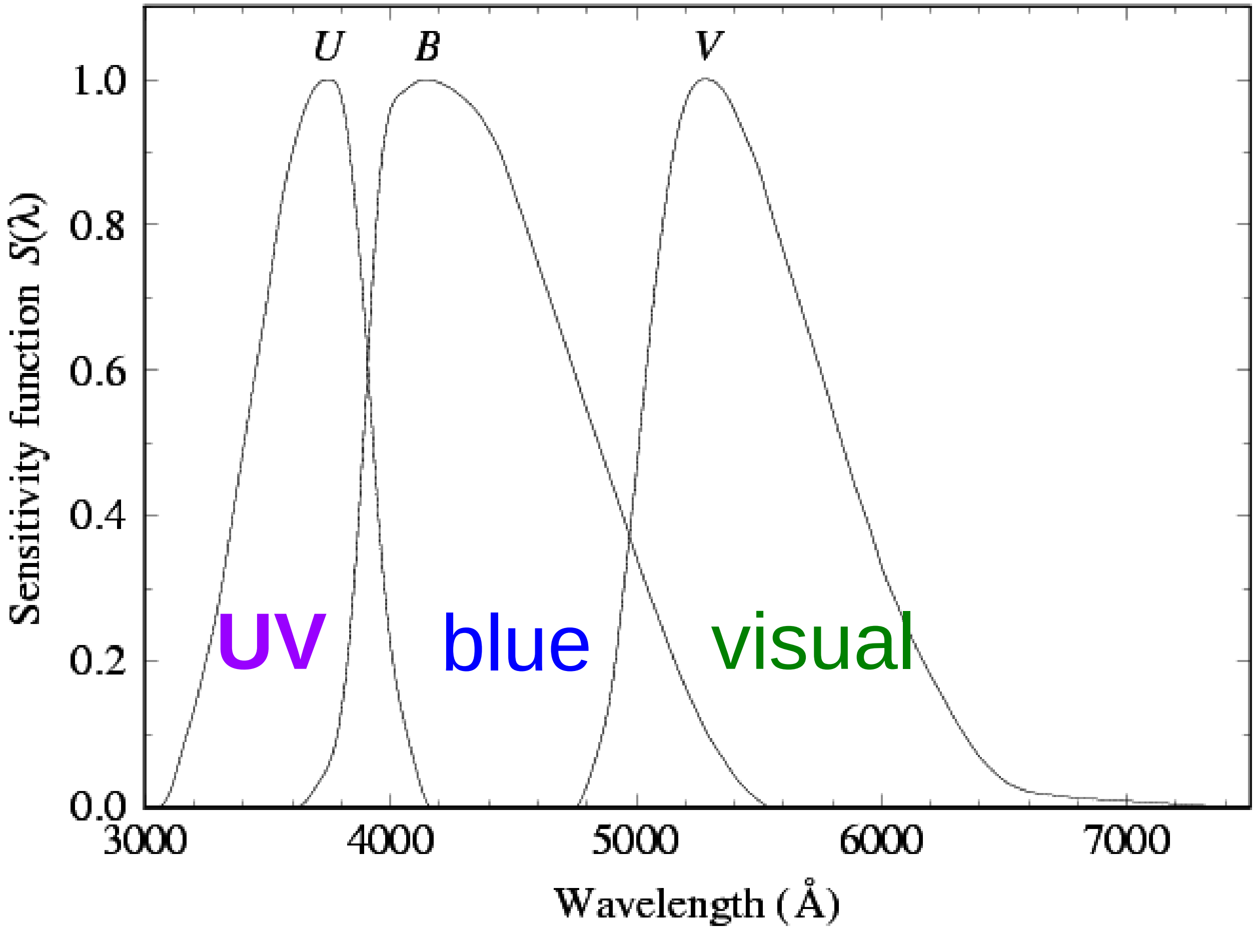

Magnitude aparente

U B V

UBV - Johnson & Morgan 1953

band	U	B	V
λ_0 (Å)	3580	4390	5450
$\frac{1}{2}\Delta\lambda$ (Å)	550	990	850

Espectro solar e sistema UBV

774 *R. A. Bell, G. Paltoglou and M. J. Tripicco*

(1994, MNRAS 268, 771)

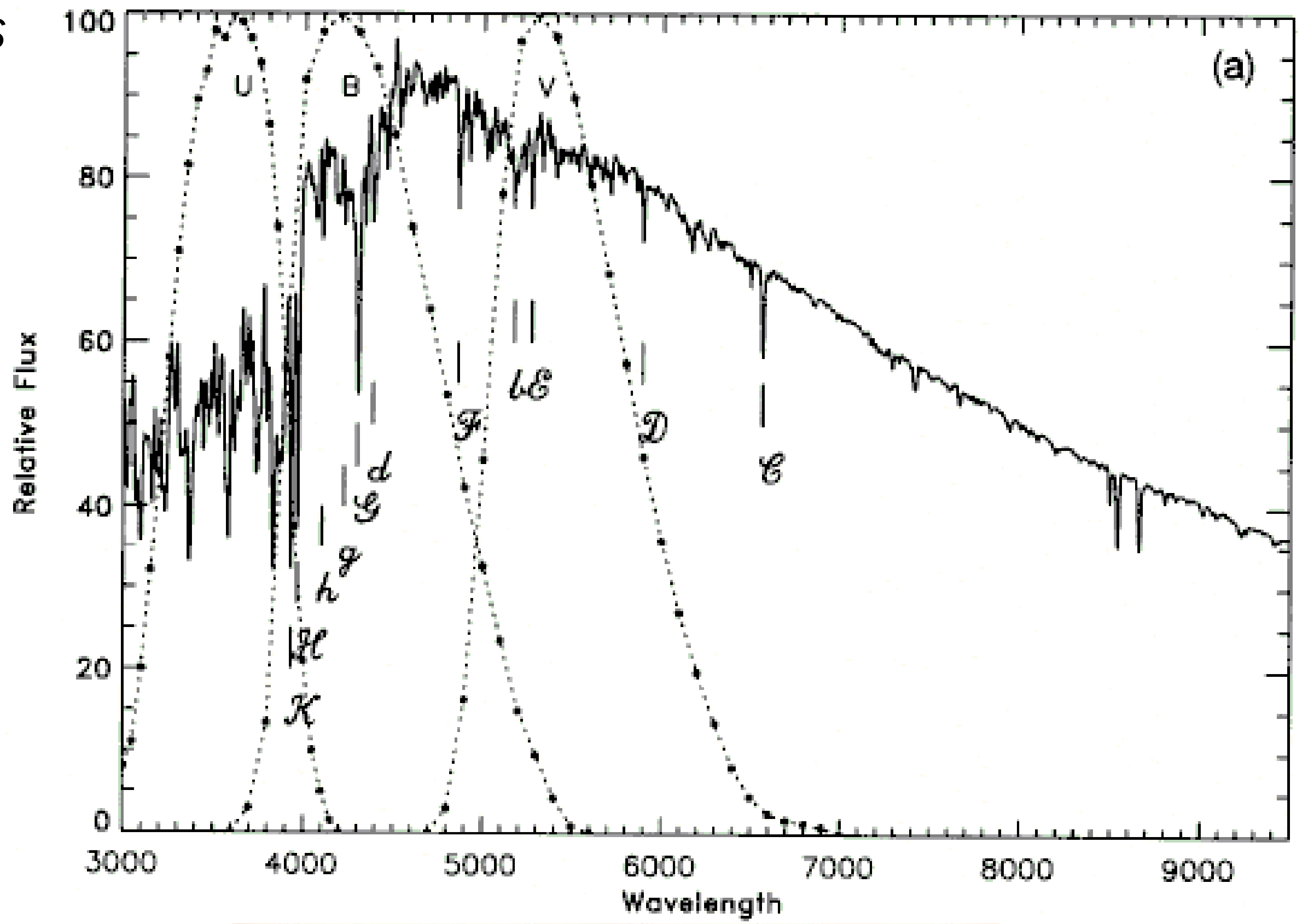

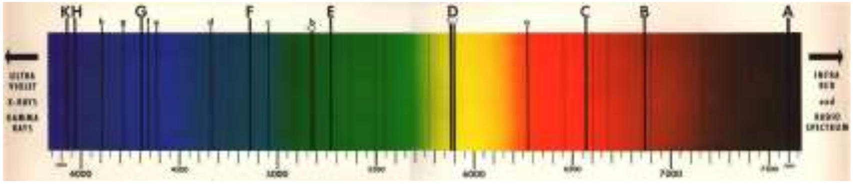

Índice de cor (ou “cor”)

Diferença entre magnitudes em duas bandas. No sistema UBV, as magnitudes m_v , m_B , m_V são denotadas como U, B, V.

Os índices de cor são:
índice B-V = B - V
índice U-B = U - B

Índice de cor

$$B_\lambda(T) = \frac{2hc^2}{\lambda^5}\frac{1}{e^{(hc/\lambda kT)} - 1}$$

B-V: Temperatura

U-B: composição química

774 *R. A. Bell, G. Paltoglou and M. J. Tripicco*

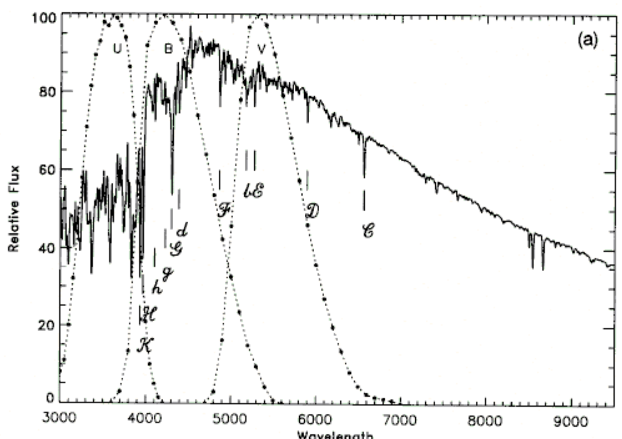

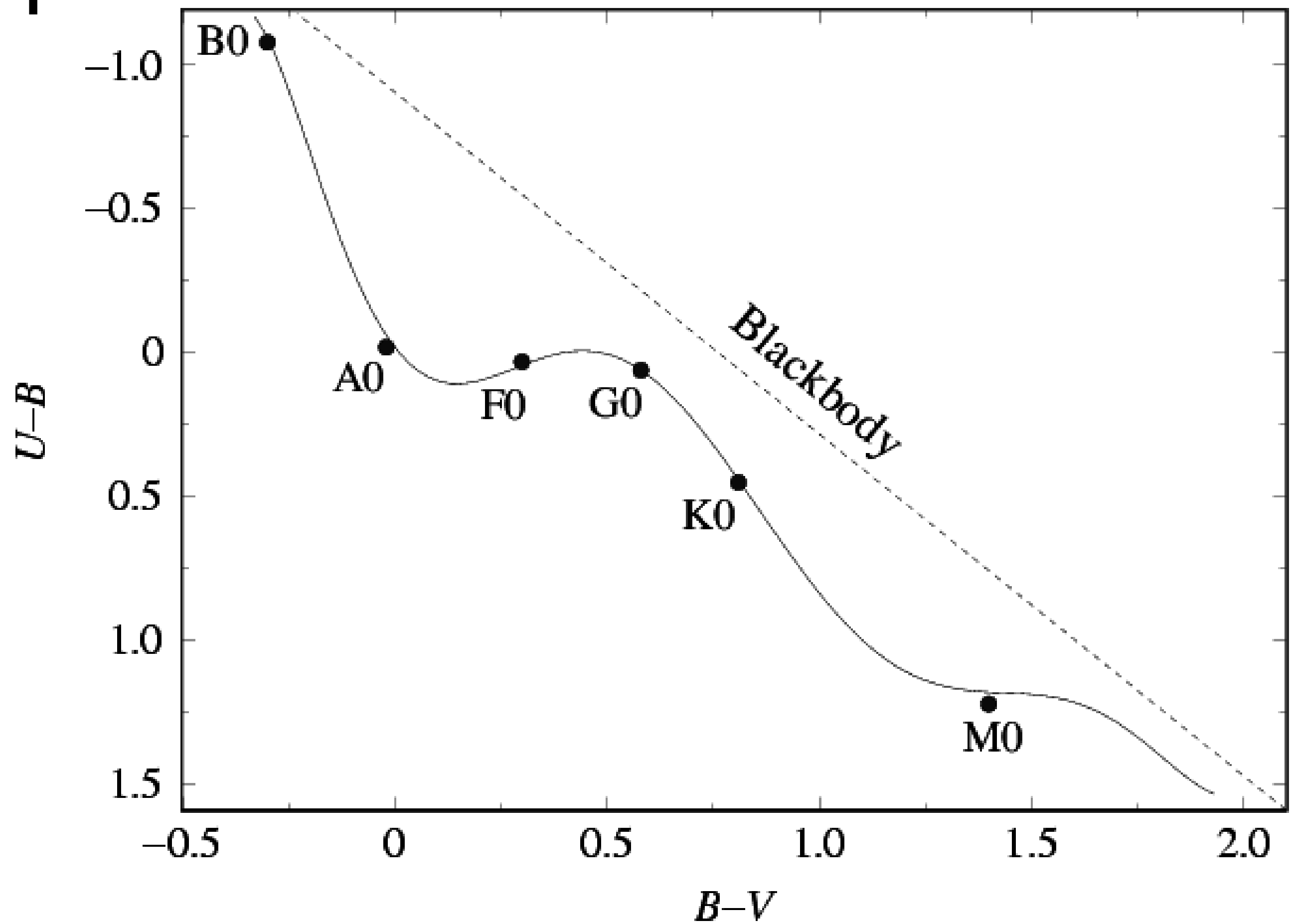

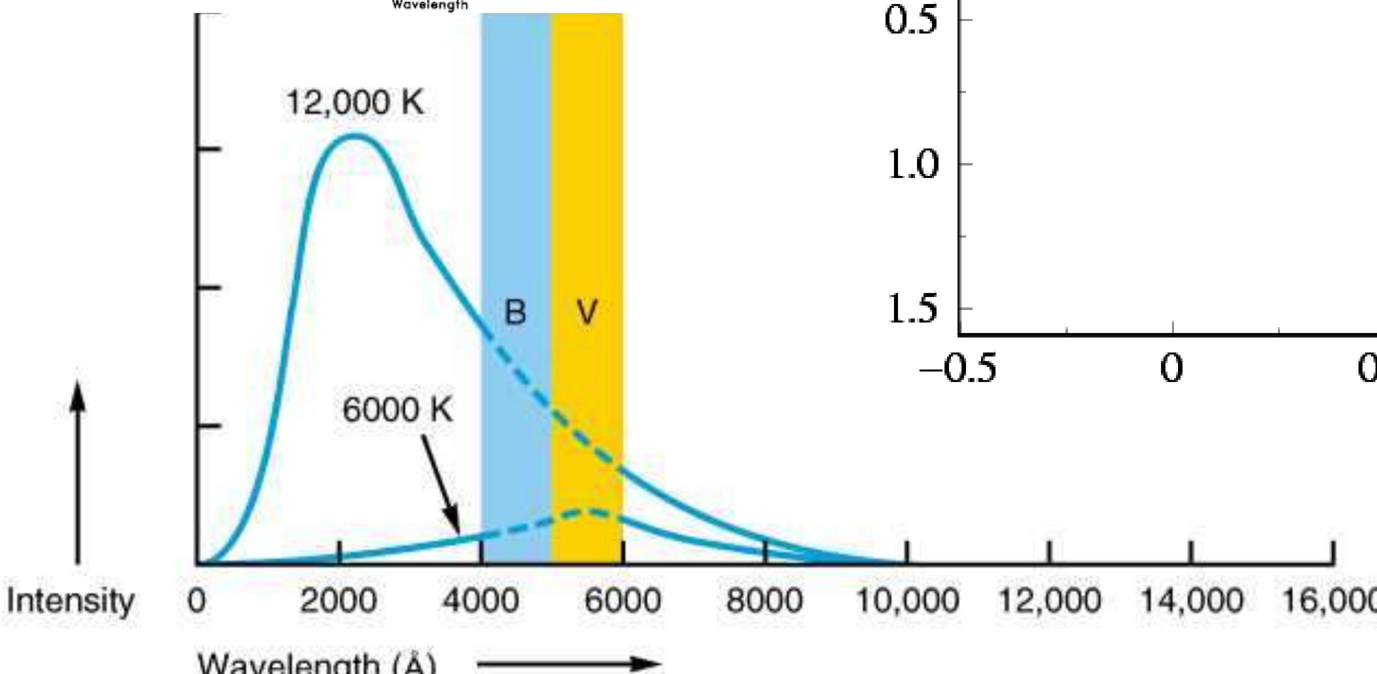

Nancy Roman, 1954, AJ, 59, 307

U-B

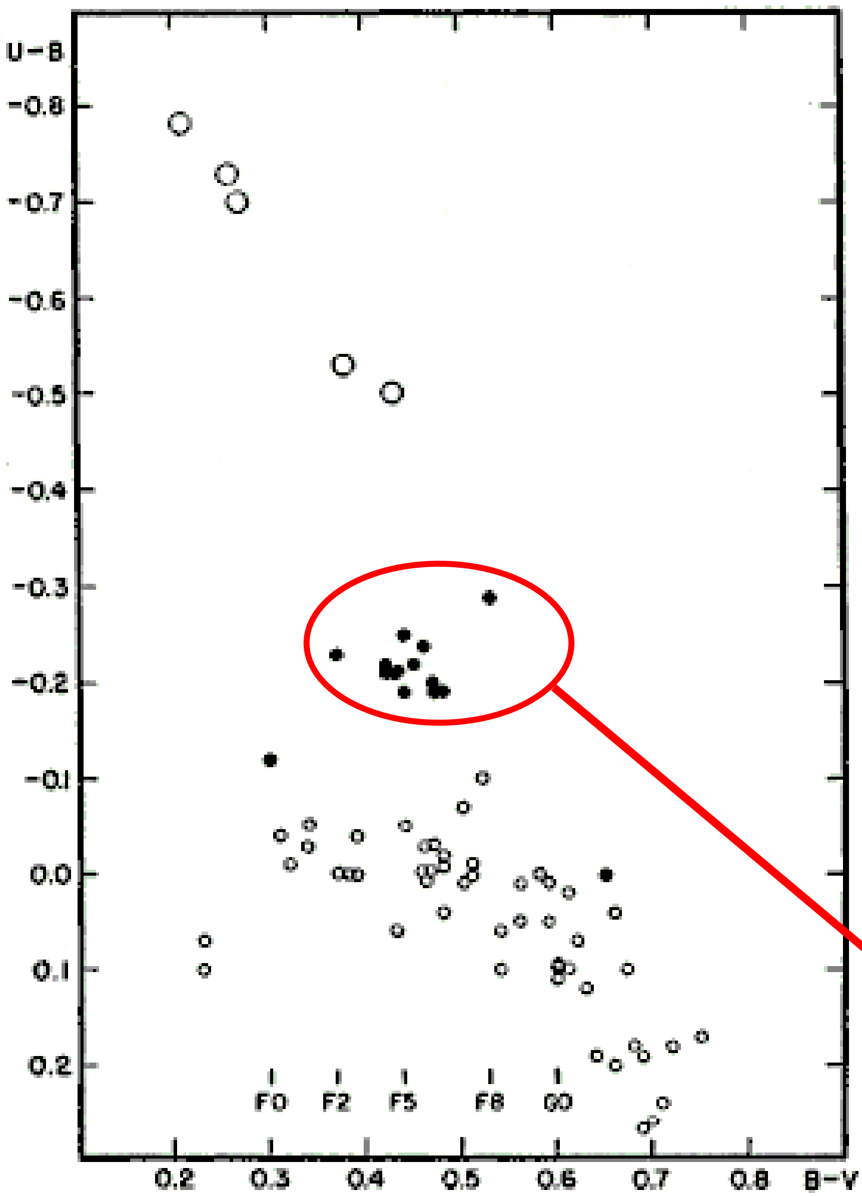

B-V

Estrelas com excesso UV

Figure 1. Two-color plot. Filled circles indicate the stars listed in Table I; small open circles are main sequence stars with *B-V* colors between +0.20 and +0.75; large open circles represent reddened O and B stars in the same range of color.

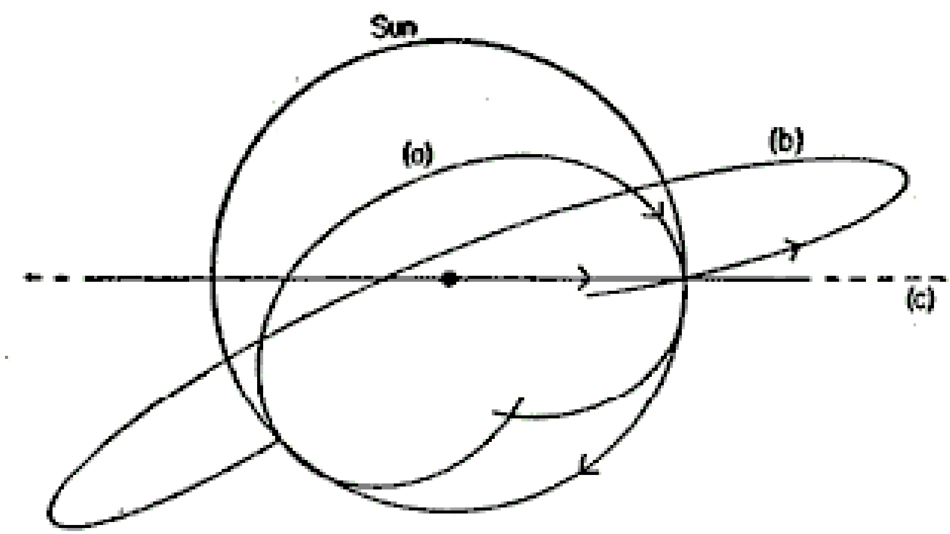

Figure 3. The orbit of the sun and portions of the orbits of (a) HD 16031, (b) BD +17°4708, and (c) BD +2°3375. For the latter three, a mean absolute magnitude of +5.0 is assumed. The scale of the diagram is given by the radii of the sun's orbit, 8.3 kpc, and of the dot at the galactic center, 200 pc. Arrows indicate the direction in which the stars move in the orbits. Notice that the stars which travel through more than one type of force field do not have closed orbits.

UV excess vs. metal deficiency

abundances of the following elements: Na, Mg, Si, Ca, Sc, Ti, Cr, Fe, and Ni. Manganese and barium have been omitted from the mean because manganese often shows an appreciable deficiency as compared with the other elements and barium is represented by only two lines and may show significant deviations from the mean. Some stars that have been analyzed by others are included in Table 1.

In Figure 1 we plot [M/H] against the ultraviolet excess. It can be seen that the correlation is good enough that the metal abundance of a main-sequence star whose color lies between $B - V = 0.45$ and 0.65 can be inferred from three-color photometry about as

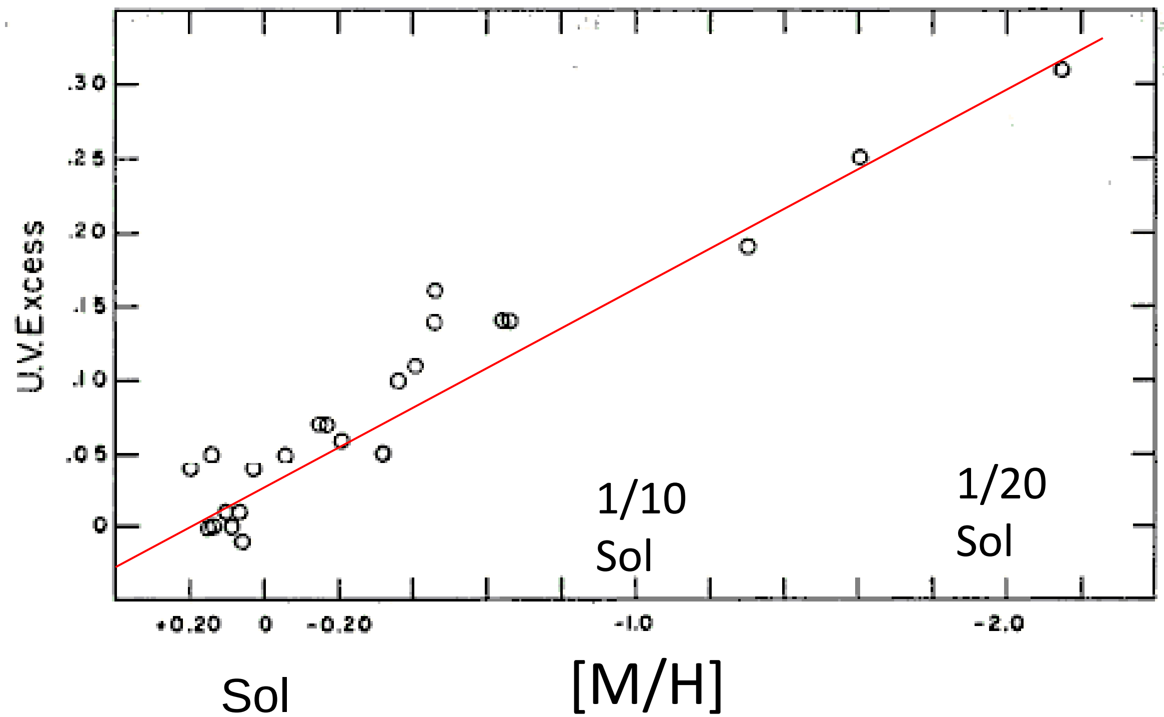

FIG. 1.—The metal deficiency plotted against ultraviolet excess for late F and early G dwarfs

well as by spectrophotometric analysis. For example, Arp (1959) has reported the ultraviolet excess of main-sequence stars ($B - V = +0.6$) in three globular clusters. For the clusters M5, M13, and M2 he quotes ultraviolet excesses of 0.21, 0.22, and 0.33 mag., respectively. Reference to Figure 1 shows that M5 and M13 are deficient in metals by a factor of about 20, while M2 must be deficient by about 200.

This material will be fully presented and more completely discussed at a later time.

GEORGE WALLERSTEIN
MAURICE CARLSON

BERKELEY ASTRONOMICAL DEPARTMENT
UNIVERSITY OF CALIFORNIA, BERKELEY

Wallerstein & Carlson 1960 ApJ 132, 276

Formação da nossa Galáxia

EVIDENCE FROM THE MOTIONS OF OLD STARS THAT THE GALAXY COLLAPSED

ELS, 1962, ApJ, 136, 748

O. J. EGGEN, D. LYNDEN-BELL,* AND A. R. SANDAGE
Mount Wilson a
Carnegie Institution of Washi

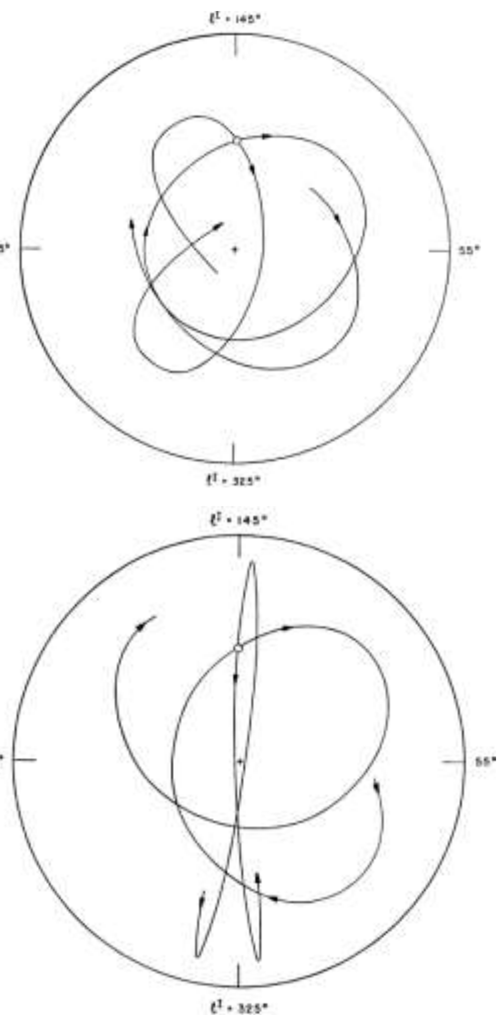

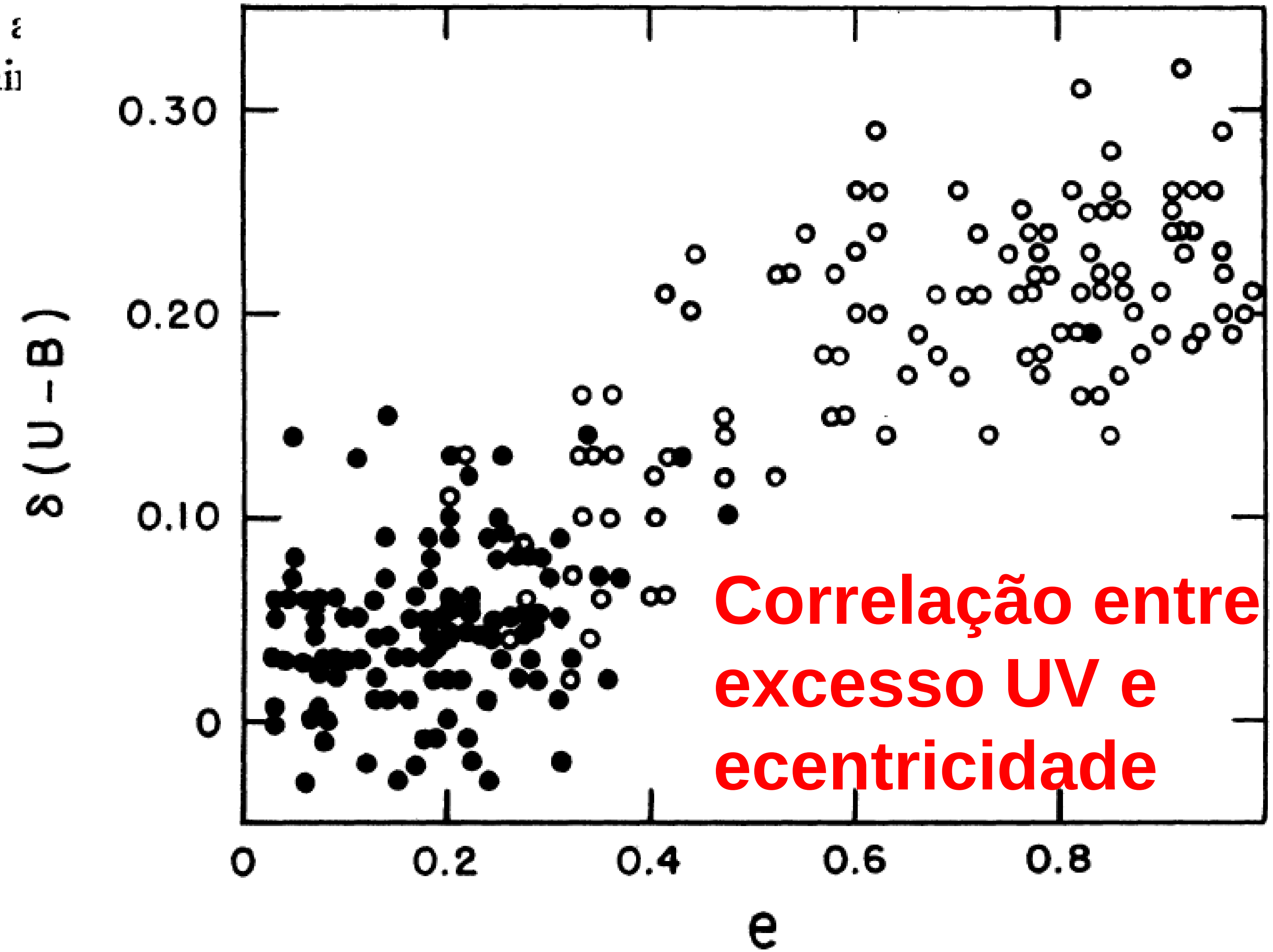

Correlação entre excesso UV e ecentricidade

Diagrama cor-magnitude

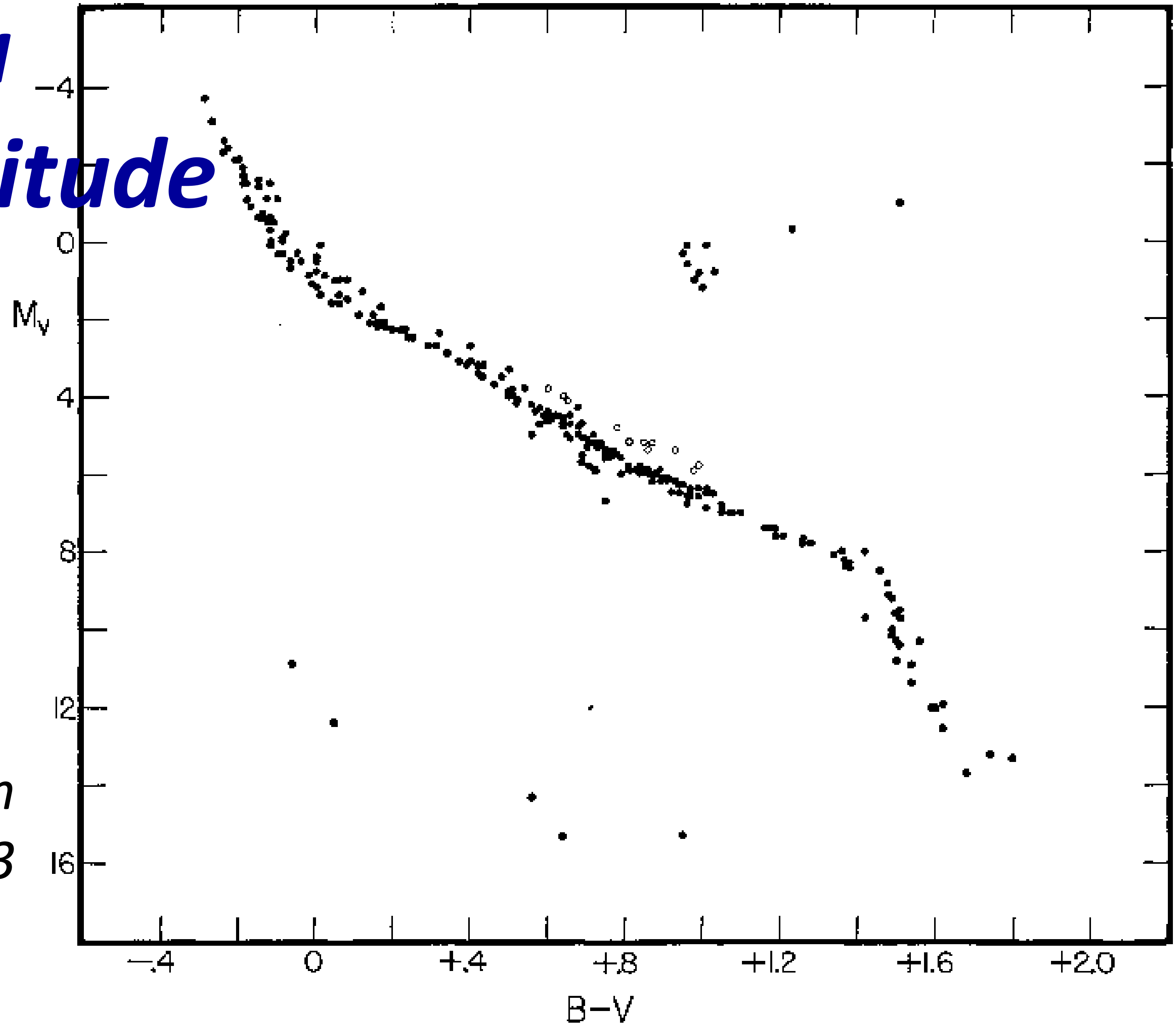

UBV

Johnson & Morgan 1953, ApJ 117, 313

FIG. 5.—A standard main sequence for the color system $B - V$ and the absolute-magnitude system M_V. The stars plotted include main-sequence objects: (*a*), which have trigonometric parallaxes ⩾ 0″100; (*b*) the Pleiades, corrected for a mean interstellar reddening (one highly reddened A star omitted); (*c*) Praesepe; (*d*) NGC 2362 corrected for a mean interstellar reddening. In addition, five white

CMD observacional e teórico

Observacional

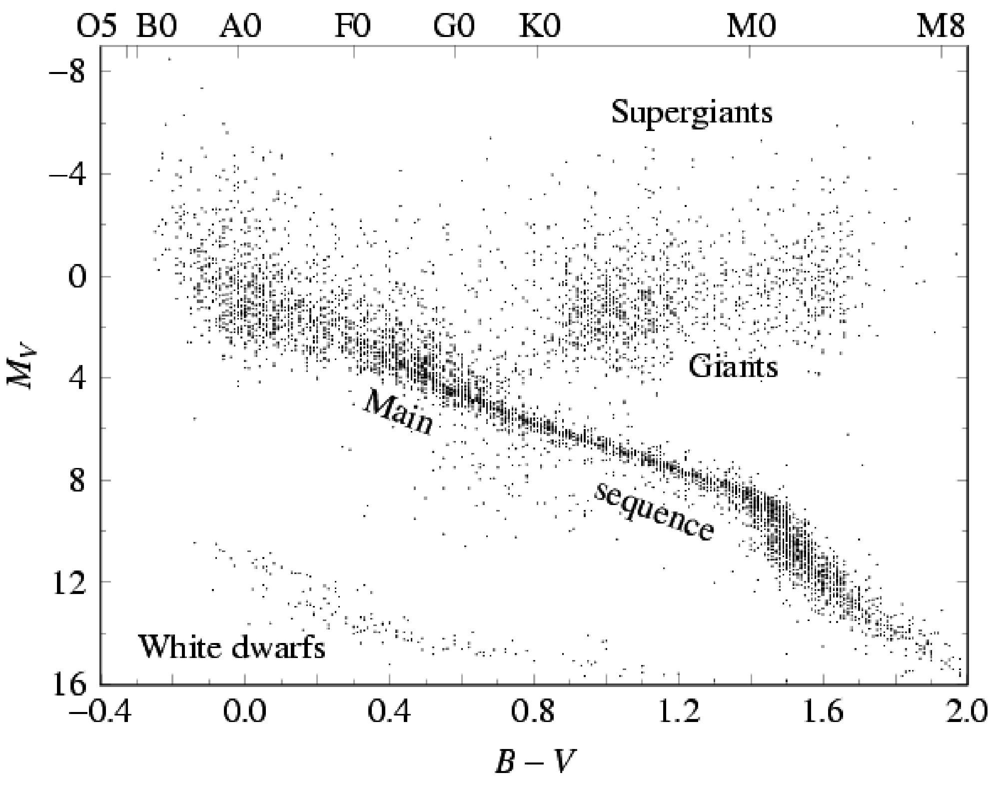

Teórico

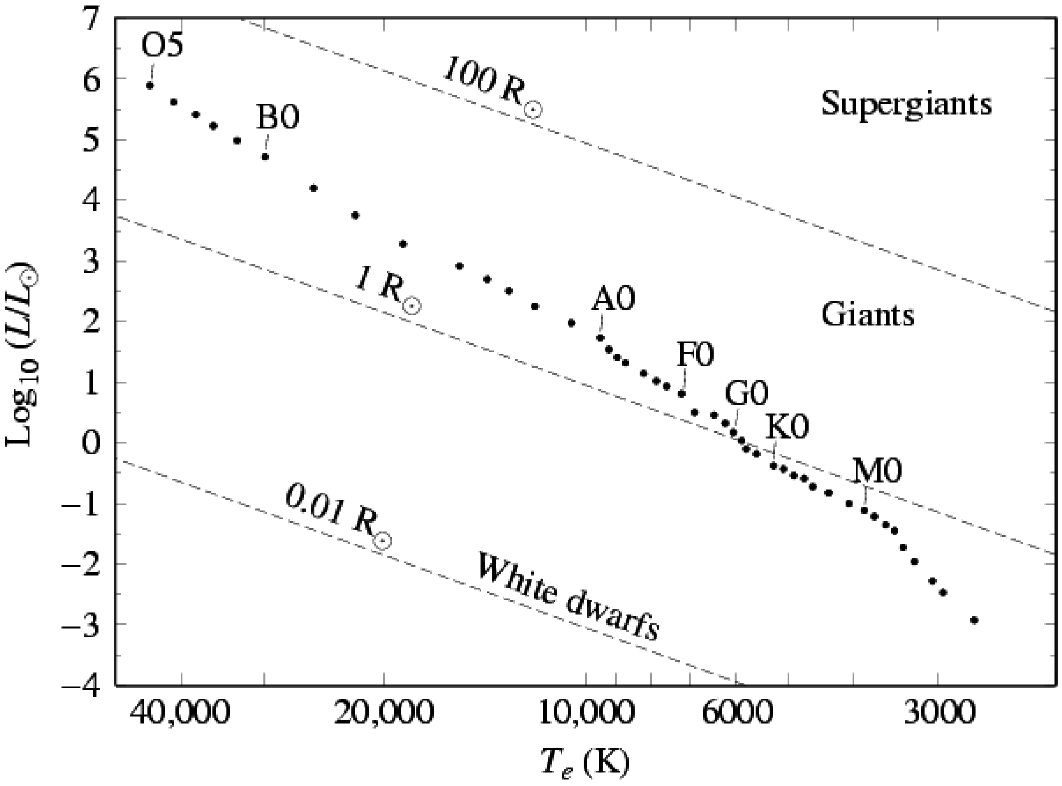

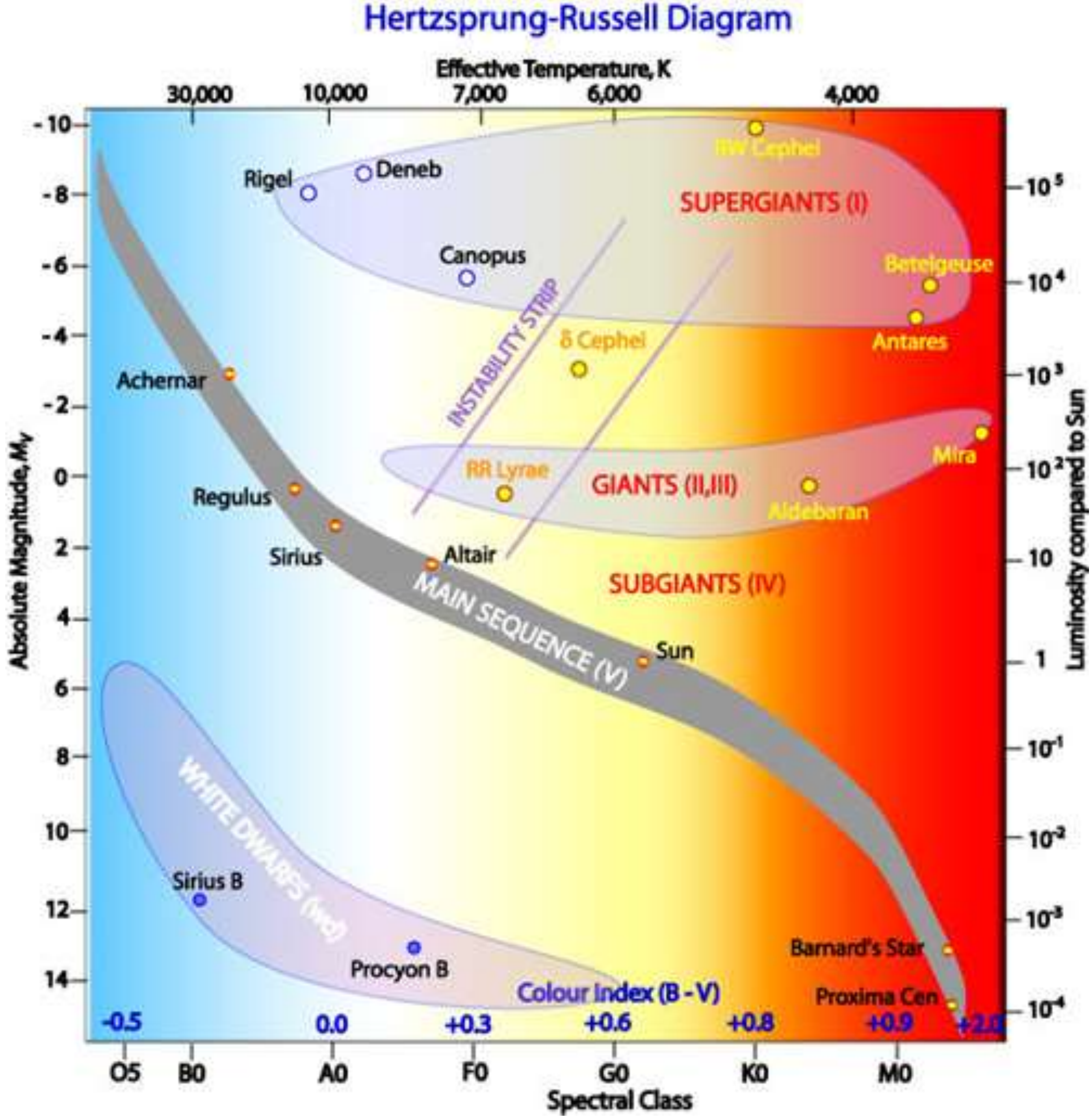

http://outreach.atnf.csiro.au/education/senior/astrophysics/stellarevolution_hrintro.html

Ponto zero do sistema UBVRI : Vega

Vega's magnitude in U-band: U = 0.0
Vega's magnitude in B-band: B = 0.0
Vega's magnitude in V-band: R = 0.0
Vega's magnitude in R-band: V = 0.0
Vega's magnitude in I-band: I = 0.0

Actually other A0 stars are used but Vega is always very close to 0.00

Normalmente os sistemas fotométricos são definidos baseados em m = 0 para Vega (ou próximo de 0)

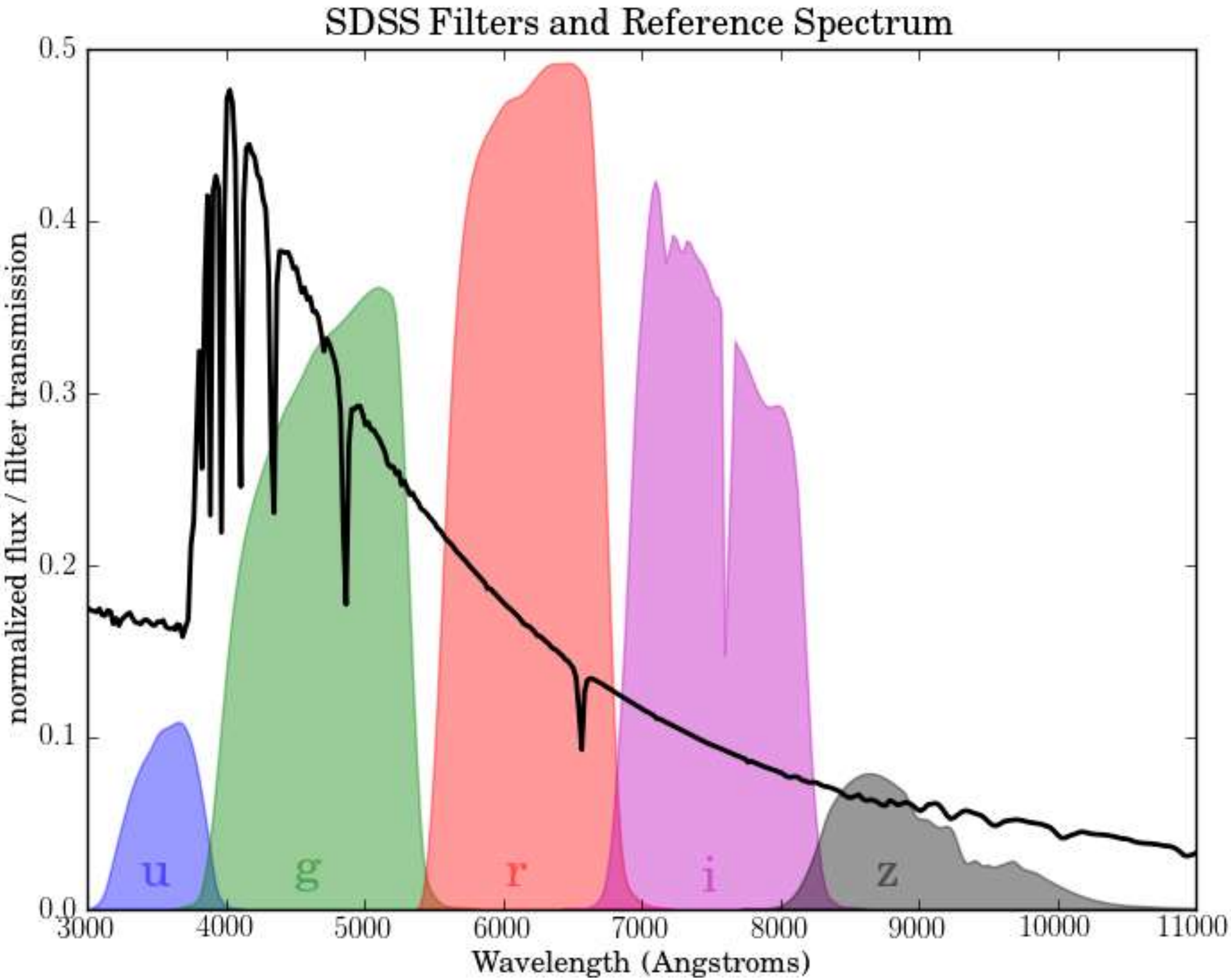

Fluxos absolutos

Fluxo para m = 0 no sistema UBVRI - JHKL

Table A2. Effective wavelengths (for an A0 star), absolute fluxes (corresponding to zero magnitude) and zeropoint magnitudes for the UBVRI JHKL Cousins-Glass-Johnson system

	U	B	V	R	I	J	H	K	Kp	L	L*
λ_{eff}	0.366	0.438	0.545	0.641	0.798	1.22	1.63	2.19	2.12	3.45	3.80
f_ν	1.790	4.063	3.636	3.064	2.416	1.589	1.021	0.640	0.676	0.285	0.238
f_λ	417.5	632	363.1	217.7	112.6	31.47	11.38	3.961	4.479	0.708	0.489
$zp(f_\lambda)$	0.770	-0.120	0.000	0.186	0.444	0.899	1.379	1.886	1.826	2.765	2.961
$zp(f_\nu)$	-0.152	-0.602	0.000	0.555	1.271	2.655	3.760	4.906	4.780	6.775	7.177

f_ν (10^{-20} ergs cm^{-2} sec^{-1} hz^{-1})

f_λ (10^{-11} ergs cm^{-2} sec^{-1} Å^{-1})

$$mag_\lambda = -2.5 \log (f_\lambda) - 21.100 - zp(f_\lambda)$$

$$mag_\nu = -2.5 \log (f_\nu) - 48.598 - zp(f_\nu)$$

Astron. Astrophys. 333, 231–250 (1998)

Model atmospheres broad-band colors, bolometric corrections and temperature calibrations for O - M stars*

M.S. Bessell[1], F. Castelli[2], and B. Plez[3,4]

Absolute fluxes

$m_1 - m_2 = -2,5 \log(f_1/f_2)$

Para m_2=0 usar os fluxos f_λ da tabela anterior, ou seja:

$$f_1 = f_\lambda\, 10^{m_1/(-2,5)}$$

$$f = f_\lambda\, 10^{-0,4m}$$

Exemplo, para Vega na banda V, m = 0, então o fluxo recebido na Terra:

$$f_V = 363,1 \times 10^{-11} \text{ erg cm}^{-2} \text{ s}^{-1} \text{ Å}^{-1}$$

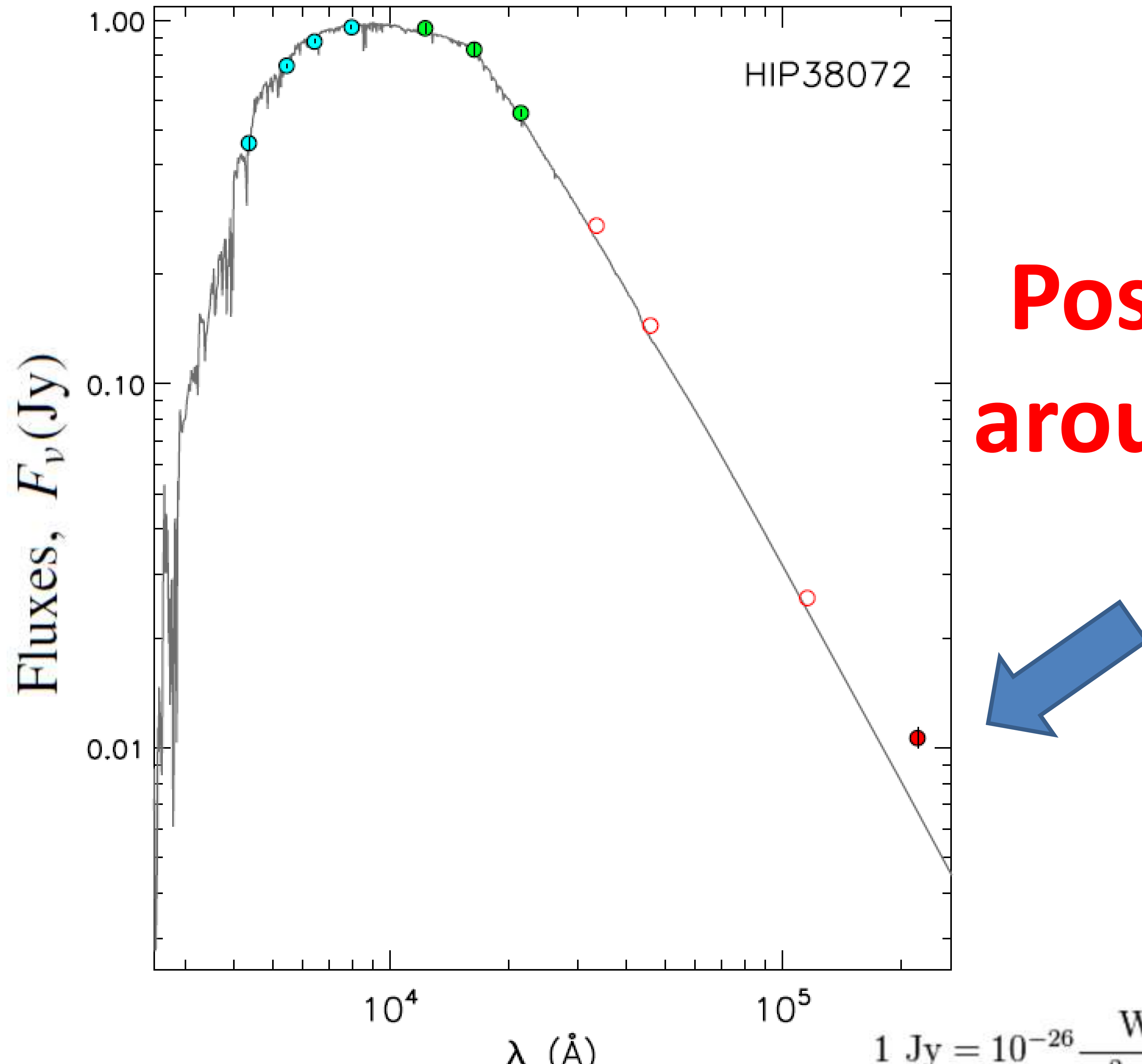

Possible disk around a solar twin?

$$1\ \mathrm{Jy} = 10^{-26}\frac{\mathrm{W}}{\mathrm{m^2\cdot Hz}}\ \text{(SI)} = 10^{-23}\frac{\mathrm{erg}}{\mathrm{s\cdot cm^2\cdot Hz}}\ \text{(cgs)}$$

THE ASTROPHYSICAL JOURNAL, 761:16 (9pp), 2012 December 10

THE INFRARED COLORS OF THE SUN

L. CASAGRANDE[1], I. RAMÍREZ[2], J. MELÉNDEZ[3], AND M. ASPLUND[1]

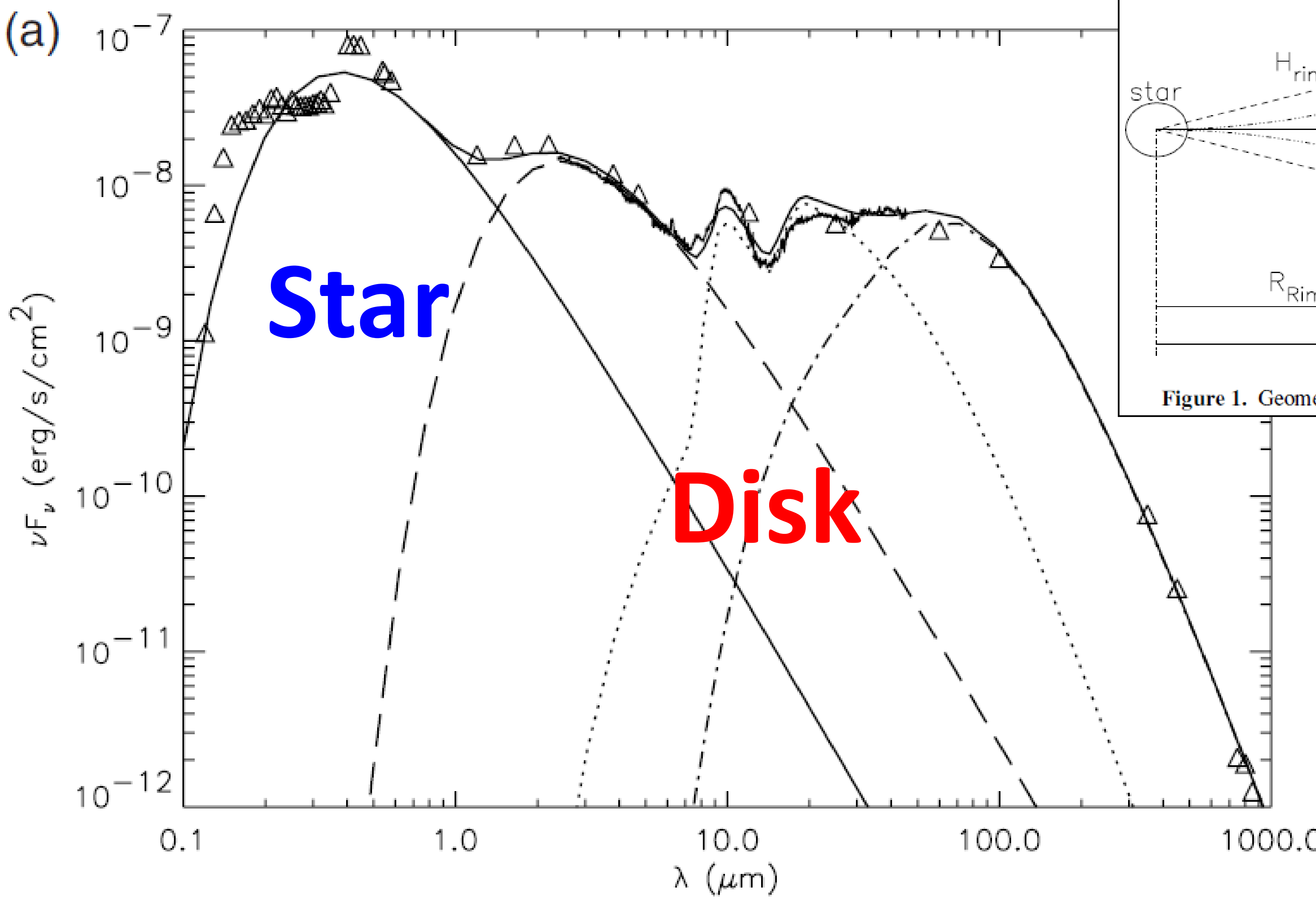

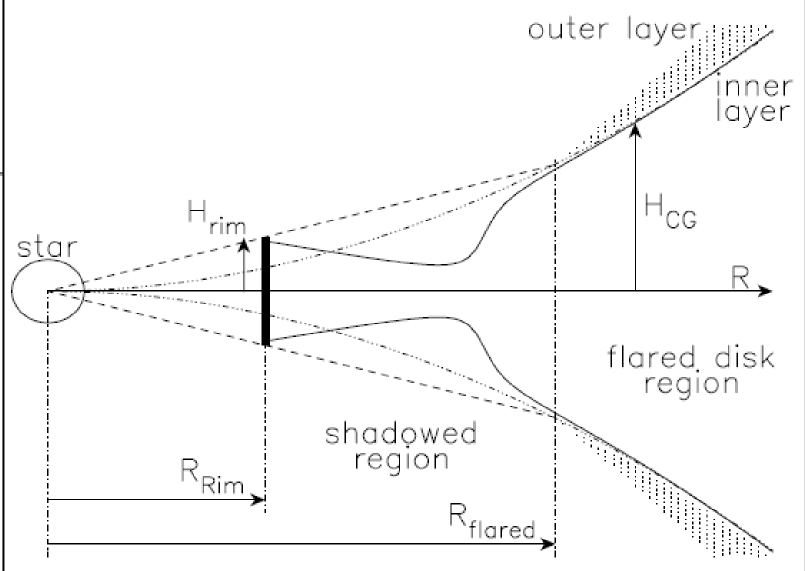

Figure 1. Geometric scheme for the model adapted from DNN01.

The use of genetic algorithms to model protoplanetary discs

Mon. Not. R. Astron. Soc. **382**, 1707–1718 (2007)

Annibal Hetem, Jr[1]★ and Jane Gregorio-Hetem★

[1] *Fundação Santo André FAFIL, Av. Príncipe de Galles, 821, Santo André, SP Brazil*

[2] *Universidade de São Paulo IAG-USP, Rua do Matão, 1226, São Paulo, SP Brazil*

Idades de aglomerados

M92

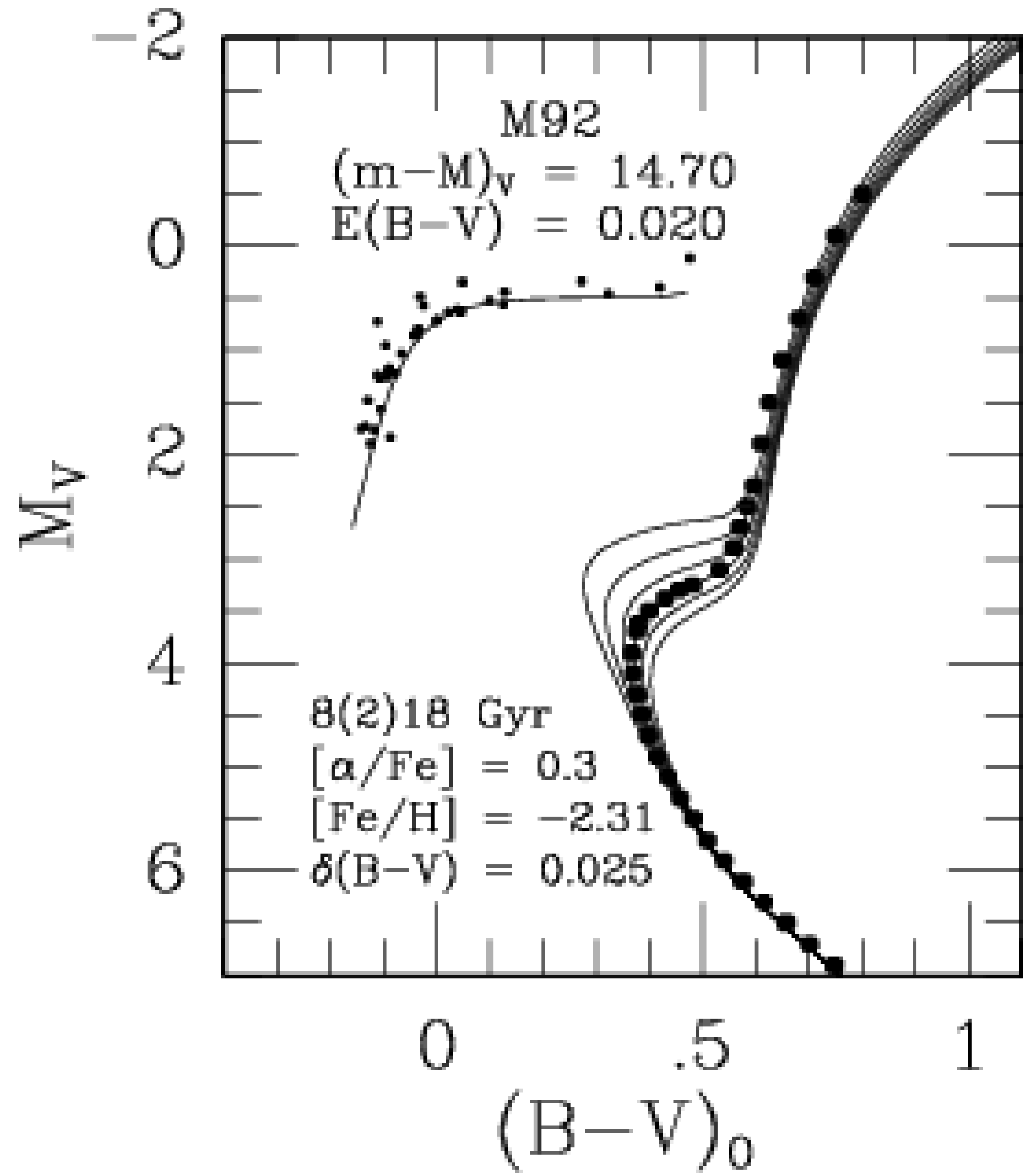

VandenBerg (2000)

Model atmospheres broad-band colors, bolometric corrections and temperature calibrations for O - M stars*

M.S. Bessell[1], F. Castelli[2], and B. Plez[3,4]

Astron. Astrophys. 333, 231–250 (1998)

Calibrações de temperatura

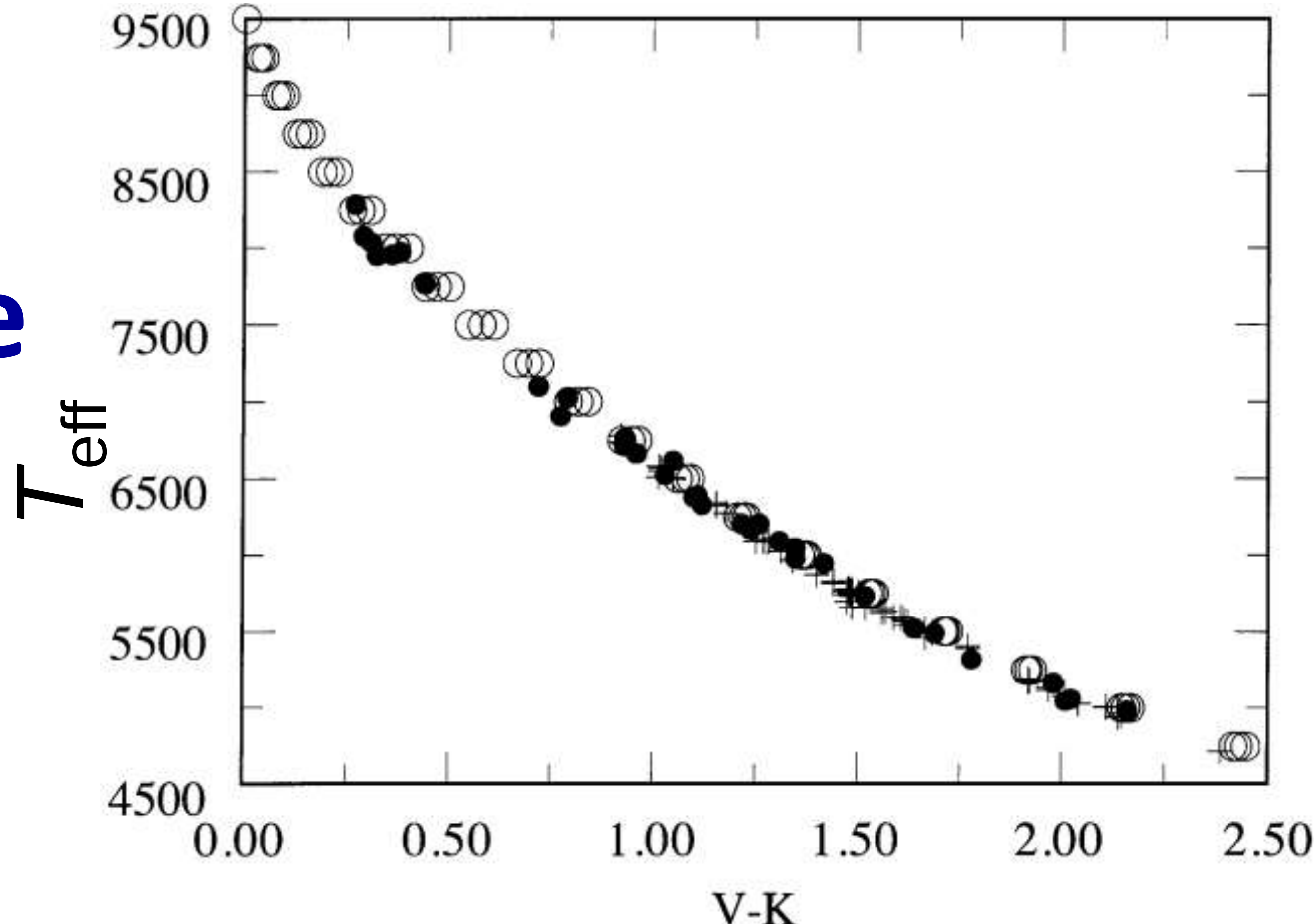

Table A3. Observed and model magnitudes and colors for the Sun and a mean solar analog

	V	U-B	B-V	V-R	V-I	V-K	J-K	H-K	Ref
Sun	-26.76								Stebbins & Kron 1957
Sun_ref	-26.75	0.128	0.649	0.370	0.726	1.511	0.372	0.039	Colina et al. 1996
Analog		0.185	0.652	0.355	0.692	1.50	0.38	0.045	Cayrel de Strobel 1996; Table 6
Model	-26.77	0.135	0.679	0.367	0.725	1.524	0.373	0.041	SUN-OVER
Model	-26.77	0.145	0.667	0.361	0.715	1.524	0.376	0.032	SUN-NOVER

A&A 512, A54 (2010)
DOI: 10.1051/0004-6361/200913204

Astronomy & Astrophysics

Calibrações melhoradas: gêmeas solares

An absolutely calibrated T_{eff} scale from the infrared flux method

Dwarfs and subgiants*

L. Casagrande[1], I. Ramírez[1], J. Meléndez[2], M. B
hing, Germa
4150-762 Po
Observatory

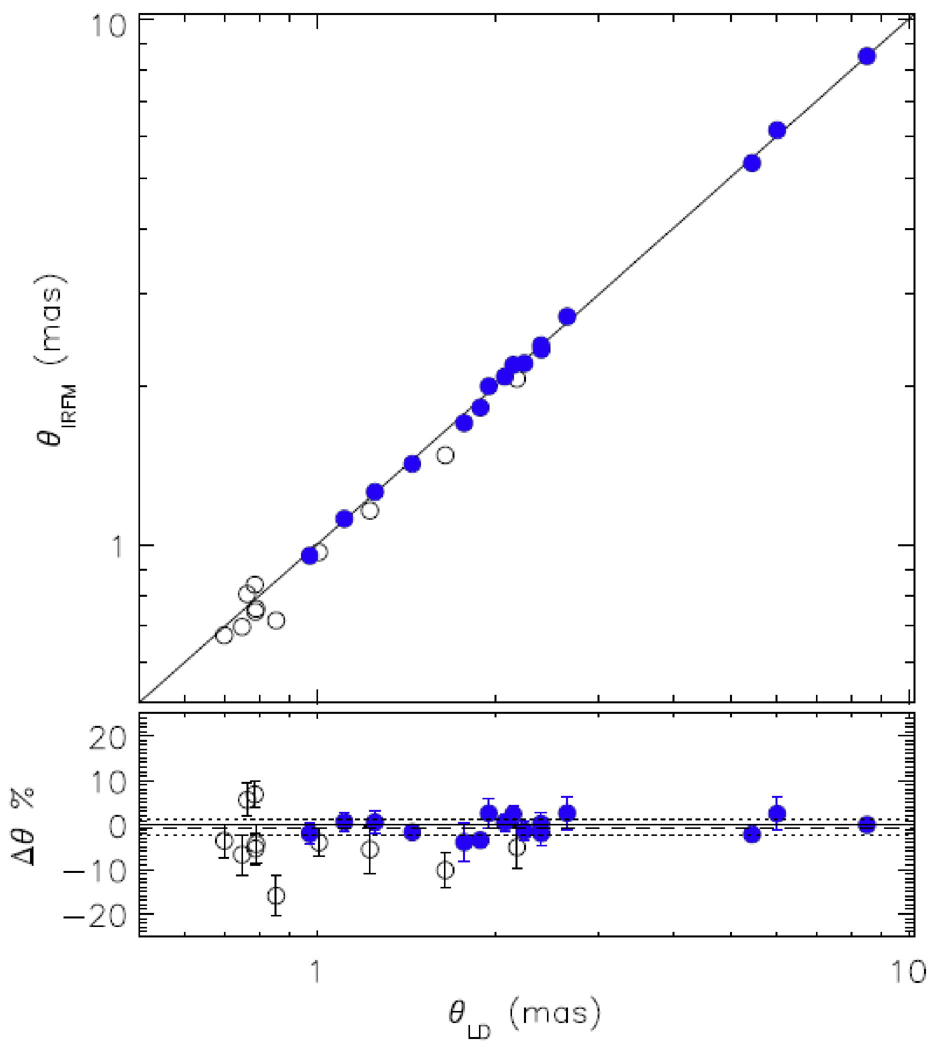

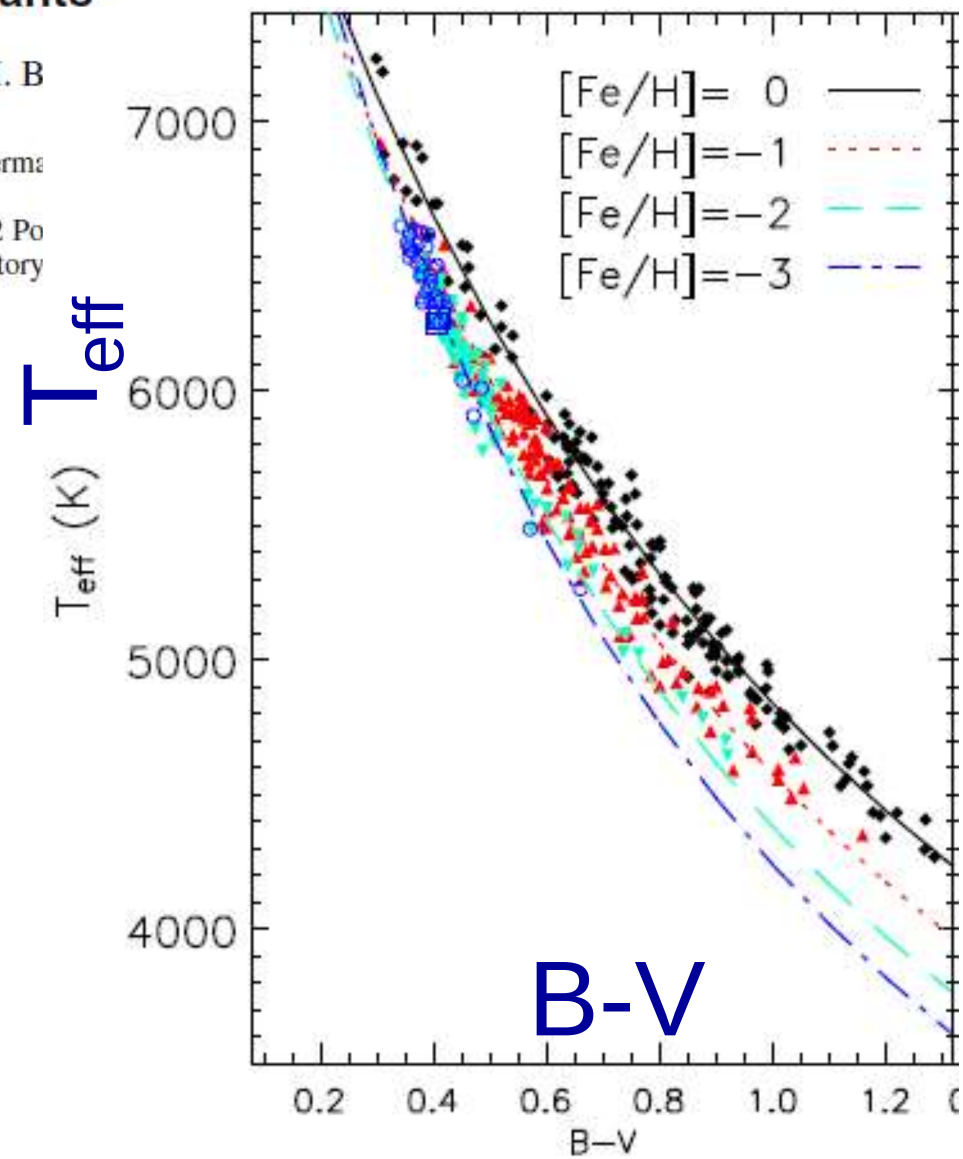

Outros sistemas fotométricos

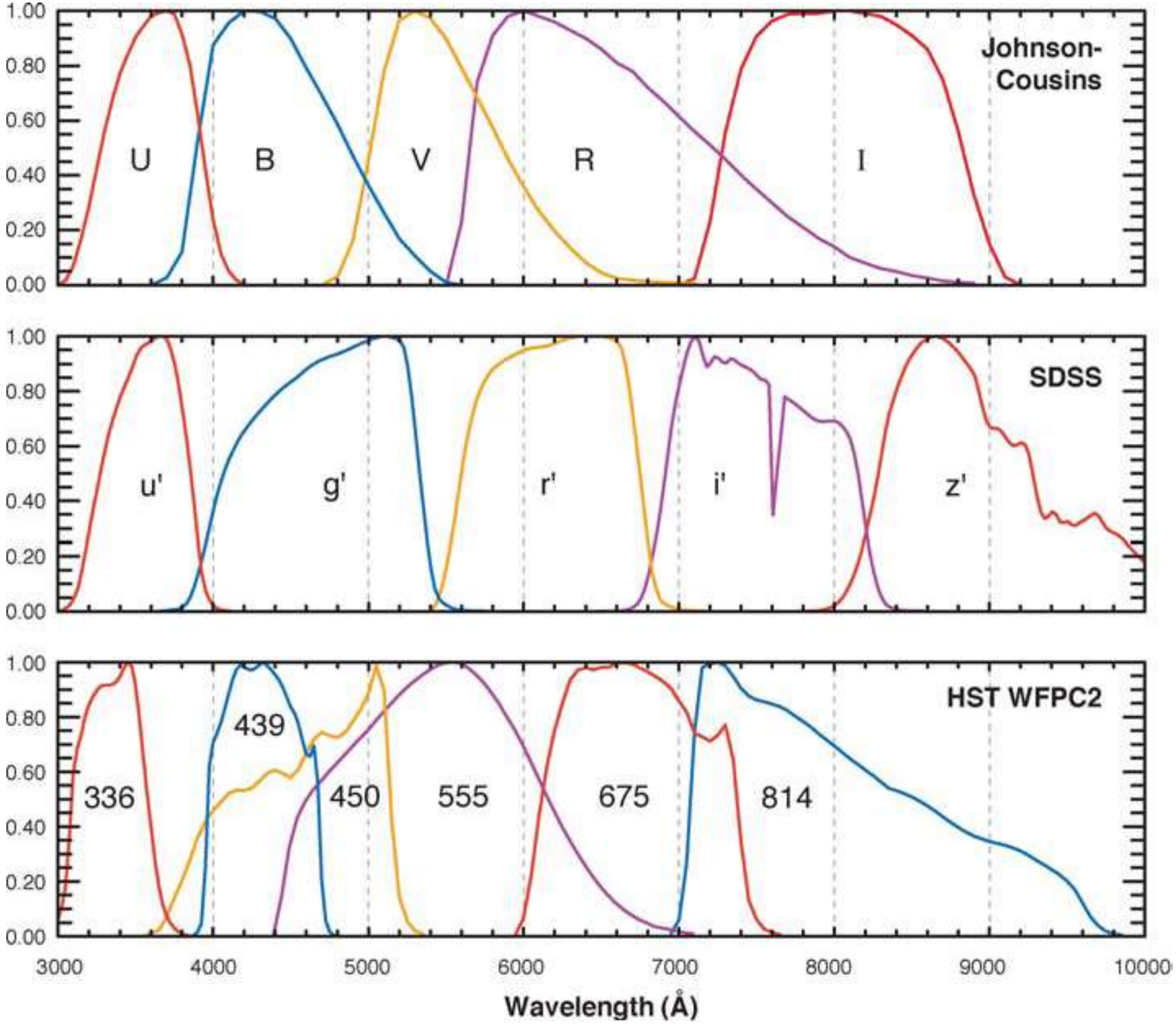

Bessell 2005, ARA&A

Outros sistemas fotométricos

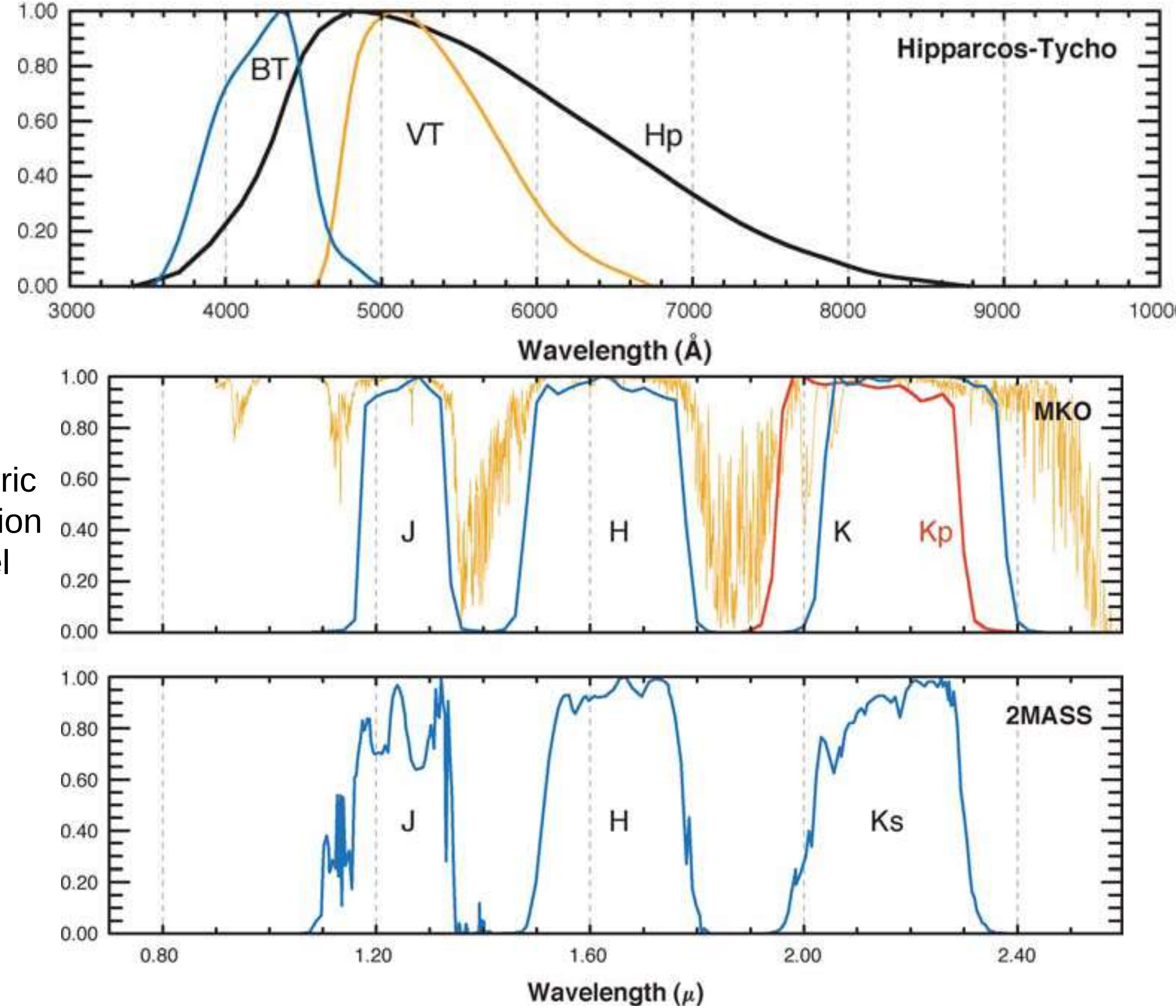

The terrestrial atmospheric transmission of a model is shown

Bessell 2005, ARA&A

A&A 512, A54 (2010)
DOI: 10.1051/0004-6361/200913204

Astronomy & Astrophysics

An absolutely calibrated $T_{\rm eff}$ scale from the infrared flux method

Dwarfs and subgiants*

L. Casagrande[1], I. Ramírez[1], J. Meléndez[2], M. Bessell[3], and M. Asplund[1]

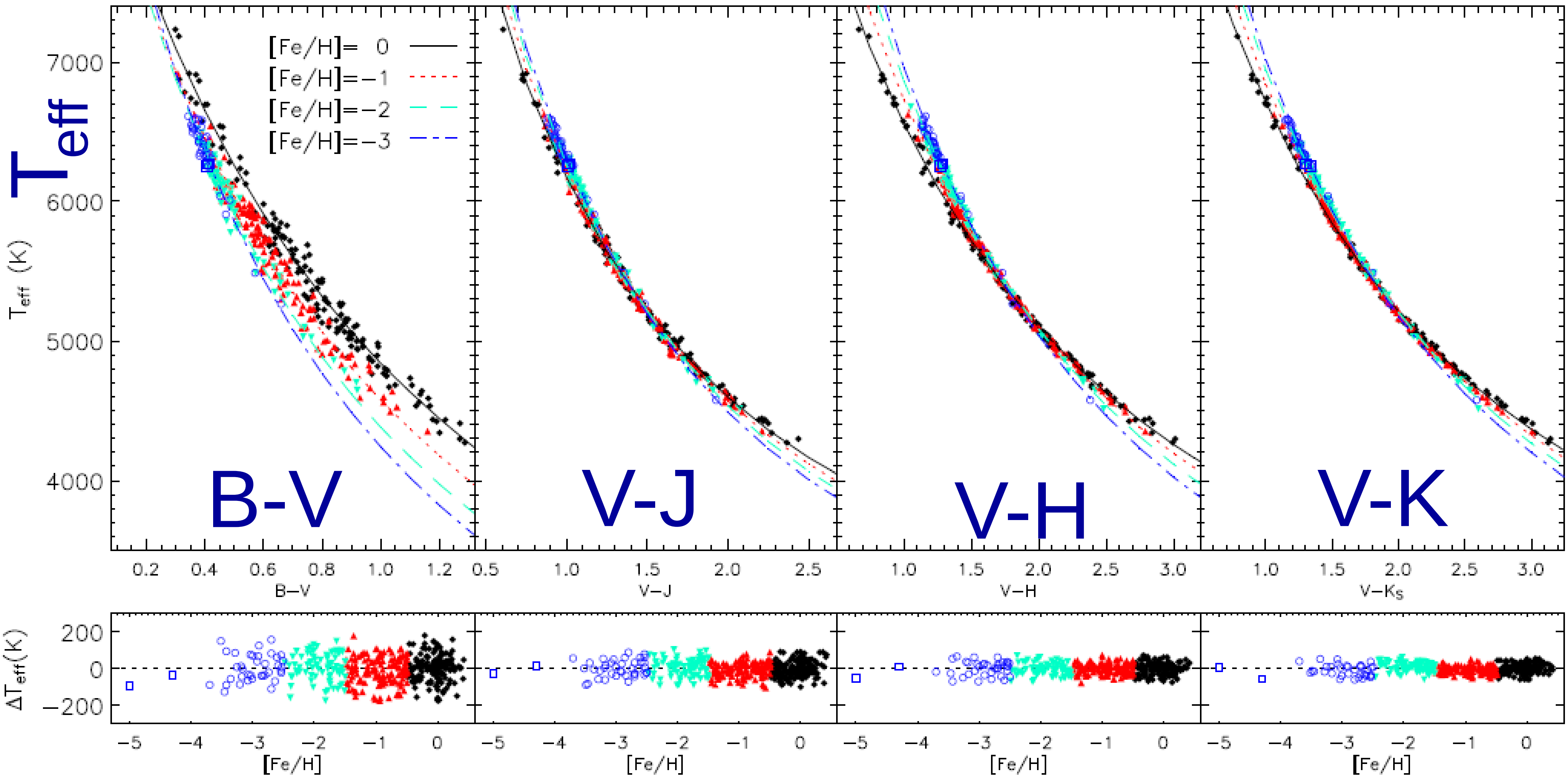

Fig. 14. Upper panels: empirical colour–temperature–metallicity calibrations in the metallicity bins $-0.5 < [Fe/H] \leq 0.5$ (filled diamonds), $-1.5 < [Fe/H] \leq -0.5$ (upward triangles), $-2.5 < [Fe/H] \leq -1.5$ (downward triangles) and $[Fe/H] \leq -2.5$ (open circles). Open squares are for the hyper metal-poor stars HE0233-0343 and HE1327-2326. Lower panels: residual of the fit as function of metallicity. For the two hyper-metal-poor stars, the residual is with respect to the fit at $[Fe/H] = -3.5$.

Effective temperature of M dwarfs

Mon. Not. R. Astron. Soc. 389, 585–607 (2008)

M dwarfs: effective temperatures, radii and metallicities

Luca Casagrande,[1★] Chris Flynn[1] and Michael Bessell[2]

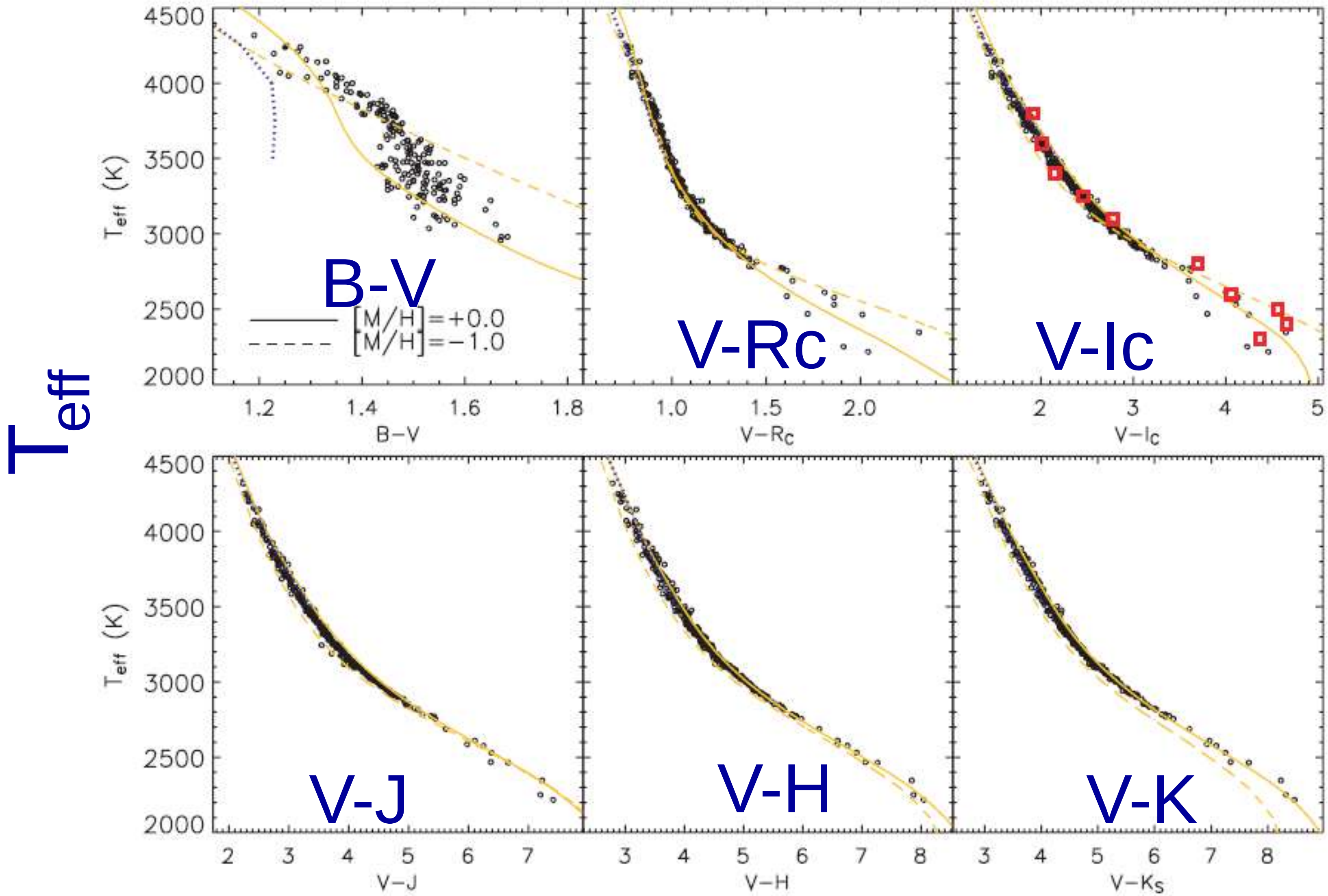

9. Colour–T_{eff} plots in different bands for our M dwarfs. Overplotted are the prediction from the Phoenix models (solid and dashed lines) for two nt metallicities which roughly bracket our sample of stars. Also shown for comparison the prediction from the Castelli & Kurucz (2003) models for ıetallicity (dotted line). Squares in the T_{eff} versus $V - I_C$ plot are from the temperature scale of Reid & Hawley (2005).

Sistemas fotométricos de banda intermediária

uvby-H$_\beta$

Strömgren & Crawford 1956

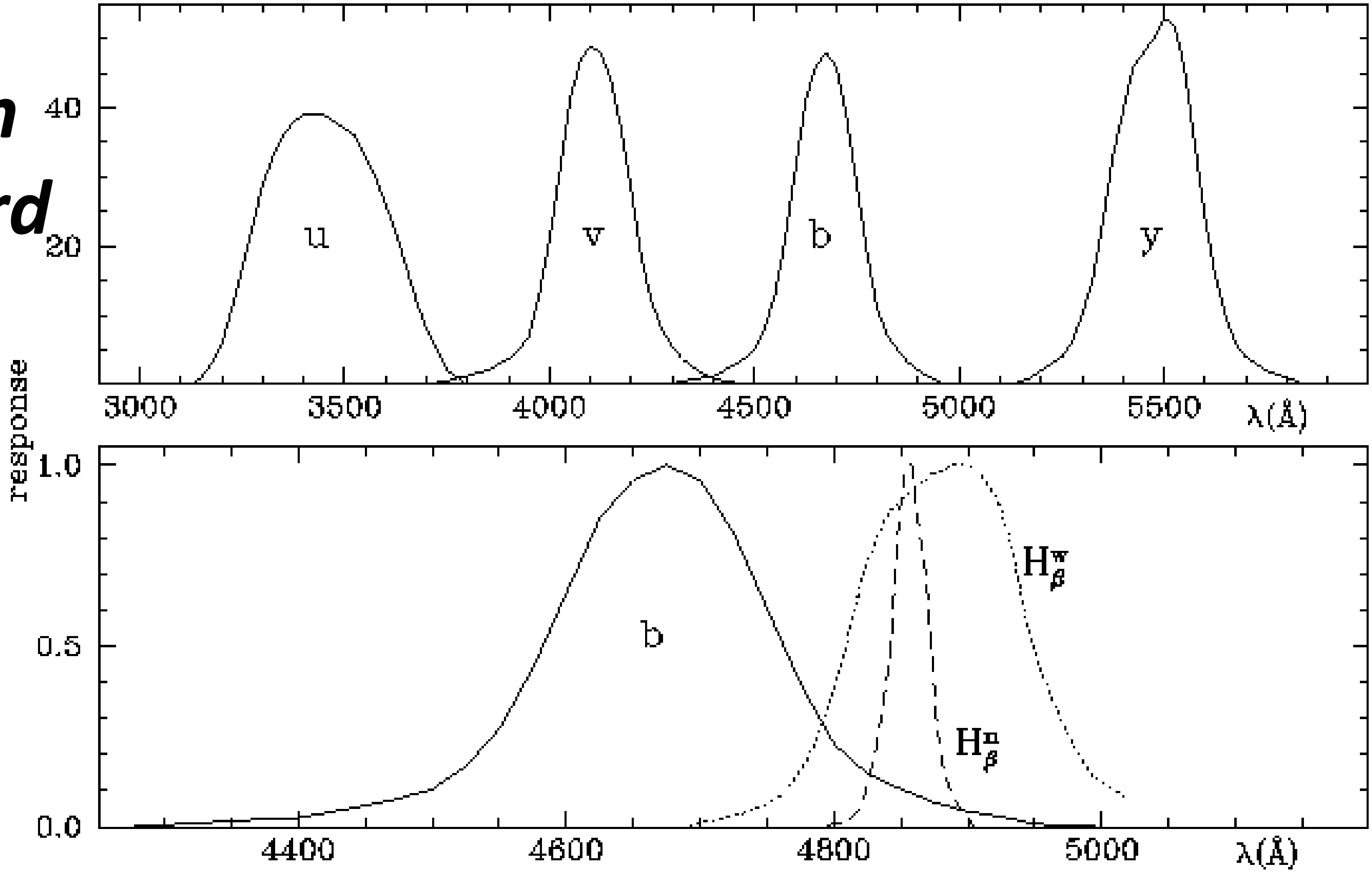

band	*u*	*v*	*b*	*y*	$H_{\beta n}$	$H_{\beta w}$
λ_{peak} (Å)	3500	4110	4670	5470	4859	4890
½Δλ (Å)	300	190	180	230	30	145

(b-y): temperatura

c_1 = (u-v) - (v-b): discont. Balmer

m_1 = (v-b) - (b-y): metalicidade

☐ 2009A&A...498..527O 1.000 05/2009 A E F D R C S O U

Önehag, A.; Gustafsson, B.; Eriksson, K.; Edvardsson, B. Calibration of Strömgren uvby-Hβ photometry for late-type stars - a model atmosphere approach

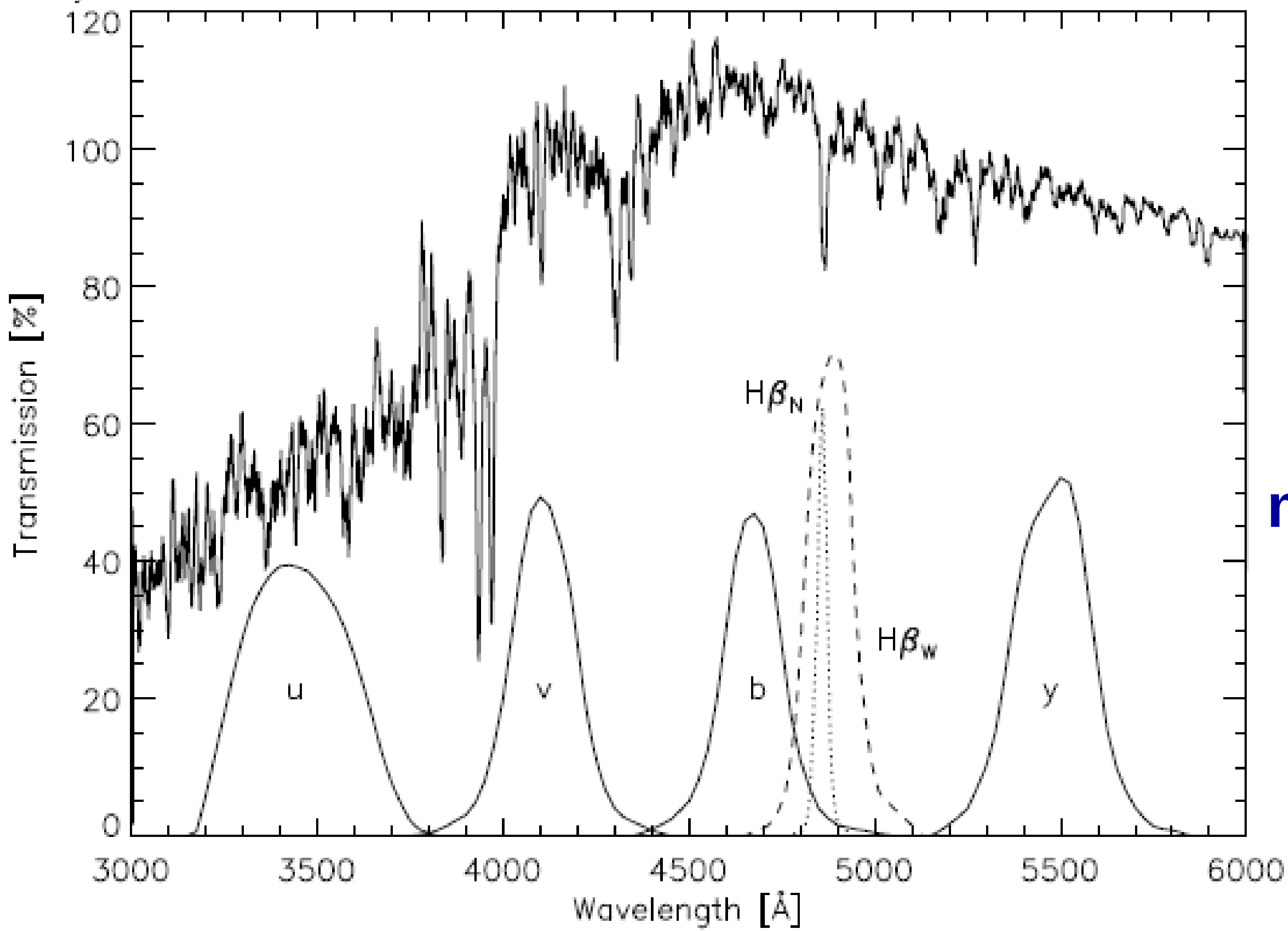

Fig. 1. The *uvby*–Hβ transmission functions of the standard systems plotted as a function of wavelength. As a comparison, the flux (per Ångström unit) of a model with $T_{\rm eff} = 6000$ K, $\log g = 4.0$ and [Me/H] = 0.0 is plotted on an arbitrary flux scale.

(b-y): Temperatura

m_1 = (v-b) - (b-y): metalicidade

ASTROPHYSICA NORVEGICA
VOL. IX NO. 31

1966, Ap. Norveiga 9, 333

ON THE CHEMICAL COMPOSITION AND KINEMATICS
OF DISC HIGH-VELOCITY STARS OF THE MAIN SEQUENCE*

Determinação de [Fe/H] usando Δm_1

BY BENGT STRÖMGREN

Hyades

$$\Delta m_1 = m_1(b-y) - m_1$$

indicates the difference in metal-hydrogen ratio of the star in question in comparison with the Hyades cluster members. A positive Δm_1 means that the metal content is low relative to that of the Hyades stars.

For the main-sequence F8–G2 stars investigated by Wallerstein [6] there is a close correlation between Δm_1 and the Fe/H ratio. Following Wallerstein we define

$$\left[\frac{\text{Fe}}{\text{H}}\right] = \log\left(\frac{\text{abundance of Fe}}{\text{abundance of H}}\right)_{\text{star}} - \log\left(\frac{\text{abundance of Fe}}{\text{abundance of H}}\right)_{\text{sun}}$$

It has been found (cf. [20]) that the Wallerstein [Fe/H] values for main-sequence stars around spectral class G0 are well represented by a linear relation

$$\left[\frac{\text{Fe}}{\text{H}}\right] = 0.3 - 12 \cdot \Delta m_1$$

and that [Fe/H] can be predicted from Δm_1 with an accuracy of about 0.1 (p. e.) for the category of stars in question.

H. Bond (1970, ApJS 22, 117): [Fe/H] = 0.16 - 13.6 Δm_1

$[Fe/H]_{uvby}$: Schuster & Nissen 1984

Schuster & Nissen 1984 (A&A 221, 65):

116 stars, $-2.6 < [Fe/H] < +0.4$

$0.37 < (b-y) < 0.59$, $0.03 < m_1 < 0.57$, $0.10 < c_1 < 0.47$

$$\mathbf{[Fe/H] = -2.0965 + 22.45\, m_1 - 53.8\, m_1^2 - 62.04\, m_1(b-y) +}$$

$$\mathbf{145.5\, m_1^2(b-y) + [\, 85.1\, m_1 - 13.8\, c_1 - 137.2 m_1^2\,]\, c_1}\ (s = 0.16\ \text{dex})$$

$[Fe/H]_{uvby}$: Ramírez & Meléndez 2005a

1. For $0.19 \le (b-y) < 0.35$, with $\sigma = 0.17$ dex,

$$[\mathrm{Fe/H}] = -4.29 - 66.0m_1 + 444.2m_1(b-y) - 782.4m_1(b-y)^2 + (0.966 - 37.8m_1 - 1.707c_1)\log\eta, \quad (6)$$

where $\eta = m_1 - [0.40 - 3.0(b-y) + 5.6(b-y)^2]$.

2. For $0.35 \le (b-y) < 0.50$, with $\sigma = 0.13$ dex,

$$[\mathrm{Fe/H}] = -3.864 + 48.6m_1 - 108.5m_1^2 - 85.2m_1(b-y) + 190.6m_1^2(b-y) + [15.7m_1 - 11.1c_1 + 17.7(b-y)]c_1. \quad (7)$$

3. For $0.50 \le (b-y)_0 \le 0.80$, with $\sigma = 0.15$ dex,

$$[\mathrm{Fe/H}] = -2.63 + 26.0m_1 - 41.3m_1^2 - 45.4m_1(b-y) + 74.0m_1^2(b-y) + 17.0m_1c_1. \quad (8)$$

Mon. Not. R. Astron. Soc. **279**, 447–458 (1996)

Importante vínculo observacional para modelos de evolução química da Galáxia

The metallicity distribution of G dwarfs in the solar neighbourhood

158 citações (1/4/2014)

H. J. Rocha-Pinto and W. J. Maciel
Instituto Astronômico e Geofísico, Av. Miguel Stefano 4200, 04301-904 São Paulo, Brazil

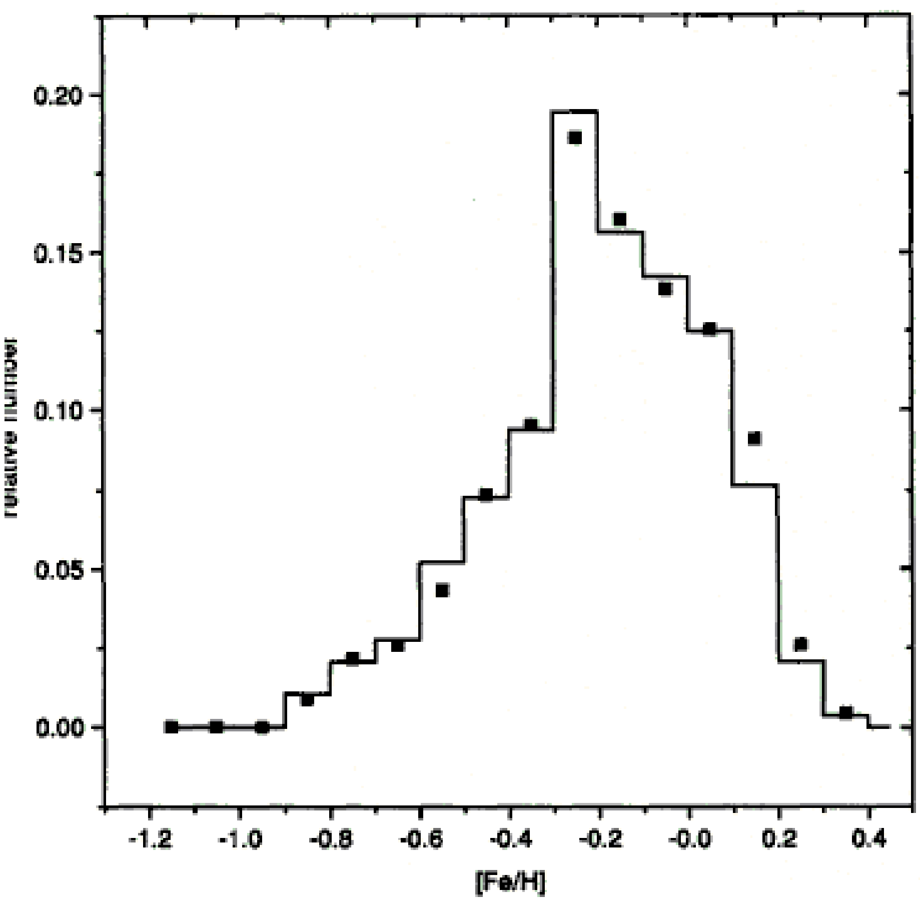

igure 2. Metallicity distribution of 287 dwarf stars with spectral types n the range G0 – G9 (continuous line), and 231 dwarfs of spectral ypes G2 – G9 (squares).

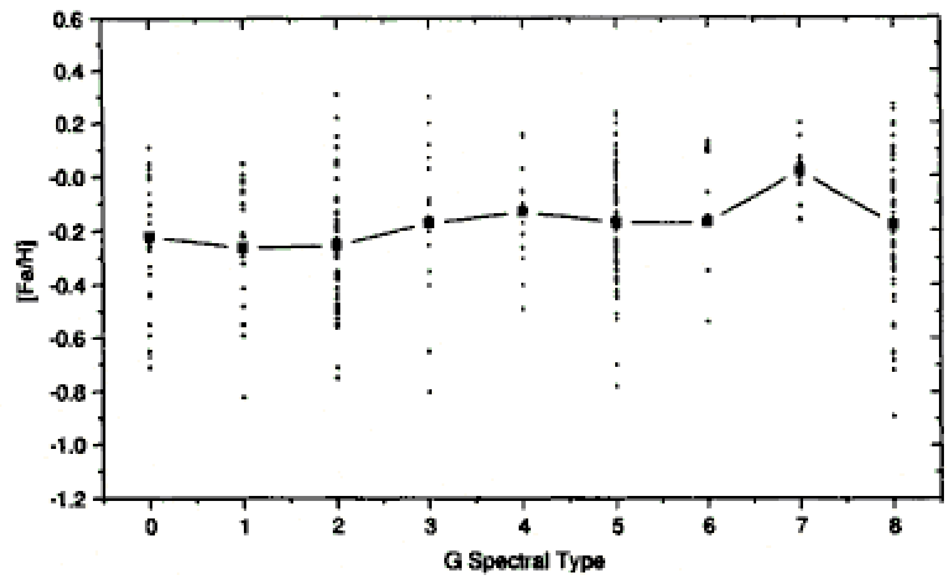

Figure 3. Abundances as a function of the spectral type (dots), and mean values for each type (squares). Stars of types G8 and G9 are merged in the same bin.

bias in the metallicity distribution, as was shown by Sommer-Larsen (1991). Since older stars generally have lower metallicities and larger scale heights relative to the galactic plane, we expect their relative number to be artificially reduced by the limitation of our sample within 25 pc of the Sun. To solve this problem, we have adopted the correction procedure introduced by Sommer-Larsen (1991), who defined a weight

Relationship between spectral type and *b-y*

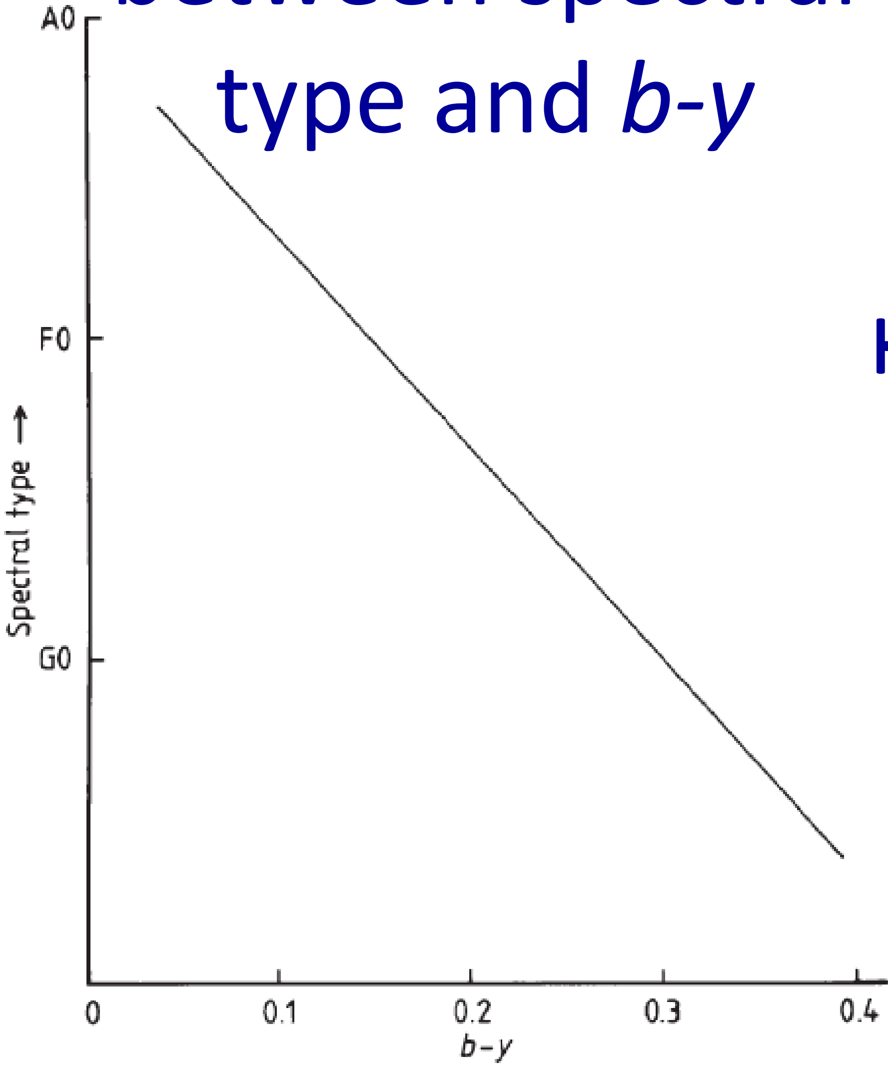

© Fig. 3.1.9, Kitchin

Relationship between T_{eff} and *b-y*

T_{eff}

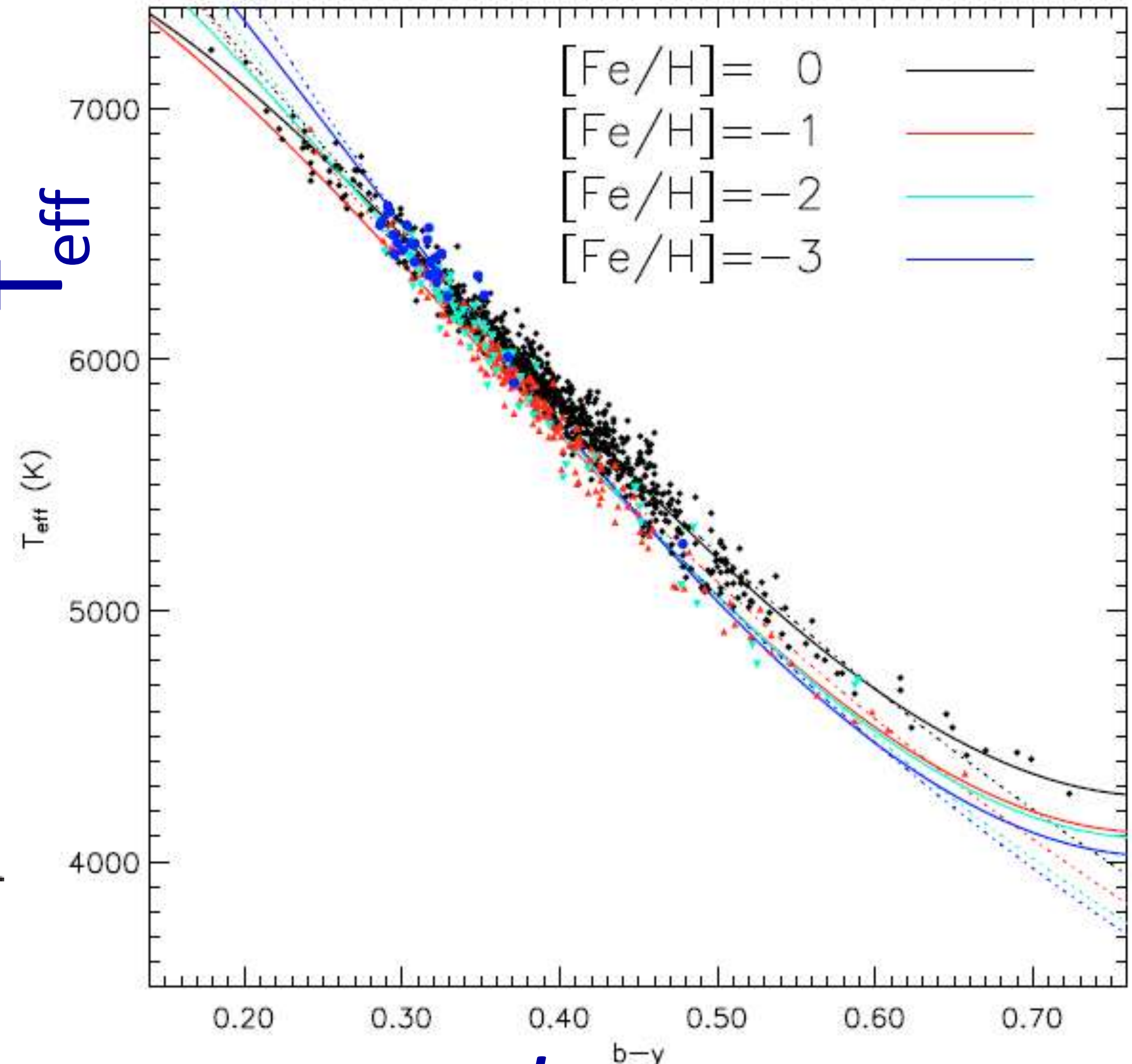

b - y

A&A 512, A54 (2010)

L. Casagrande[1], I. Ramírez[1], J. Meléndez[2], M. Bessell[3], and M. Asplund[1]

Descobrindo planetas com fotometria

THE ASTROPHYSICAL JOURNAL, 529:L41–L44, 2000 January 20

A TRANSITING "51 PEG–LIKE" PLANET[1]

GREGORY W. HENRY,[2] GEOFFREY W. MARCY,[3] R. PAUL BUTLER,[4] AND STEVEN S. VOGT[5]
Received 1999 November 18; accepted 1999 December 3; published 1999 December 16

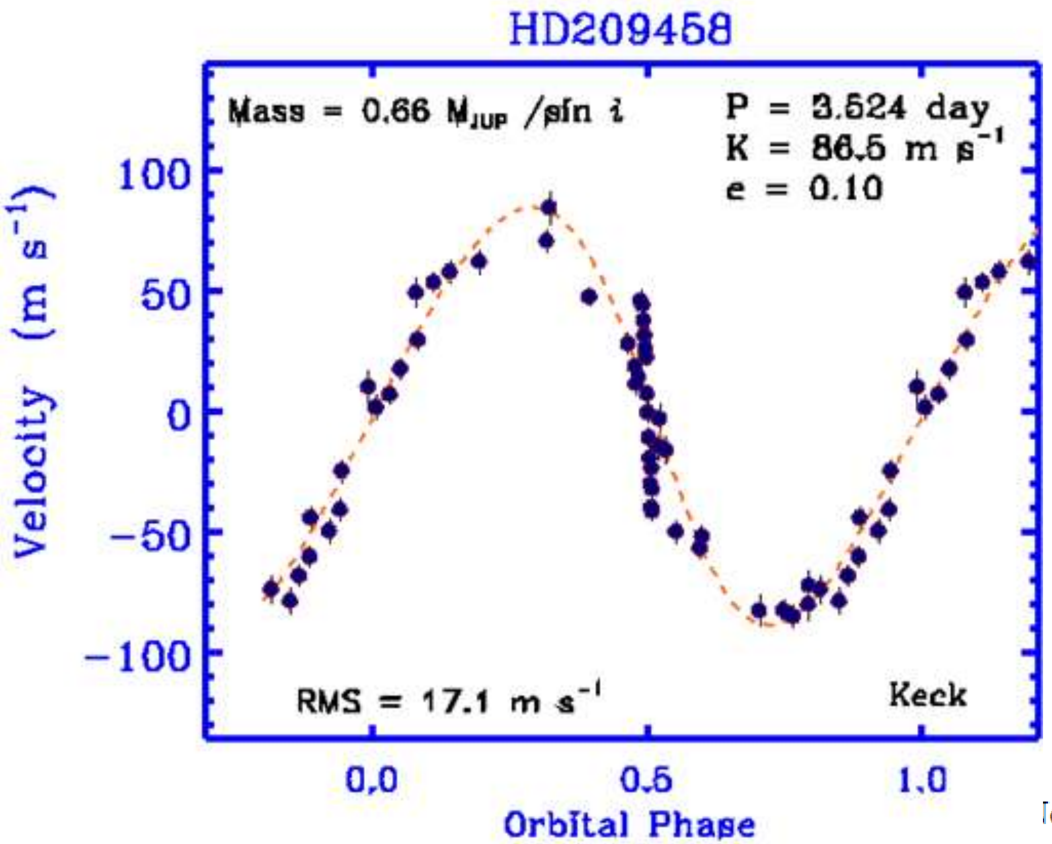

Apenas meio trânsito!

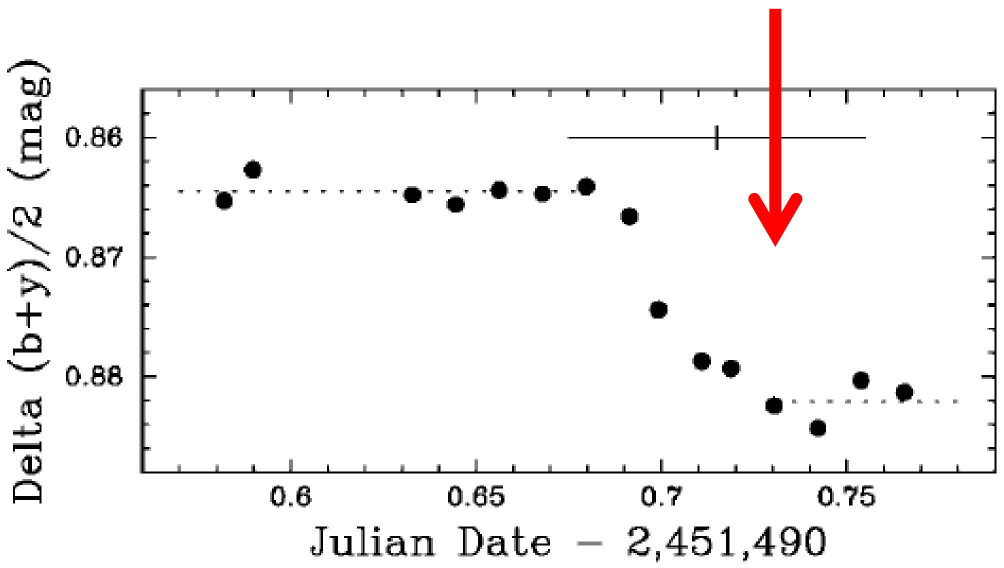

FIG. 3.—Photometric observations of HD 209458 from the night of 1999 November 7 UT showing ingress of the planetary transit. The measured transit depth is 0.017 ± 0.002 mag or 1.58% ± 0.18%. The error bar shows the time of inferior conjunction and its uncertainty predicted from the radial velocities in this Letter.

O primeiro planeta identificado com a técnica de transitos: HD 209458

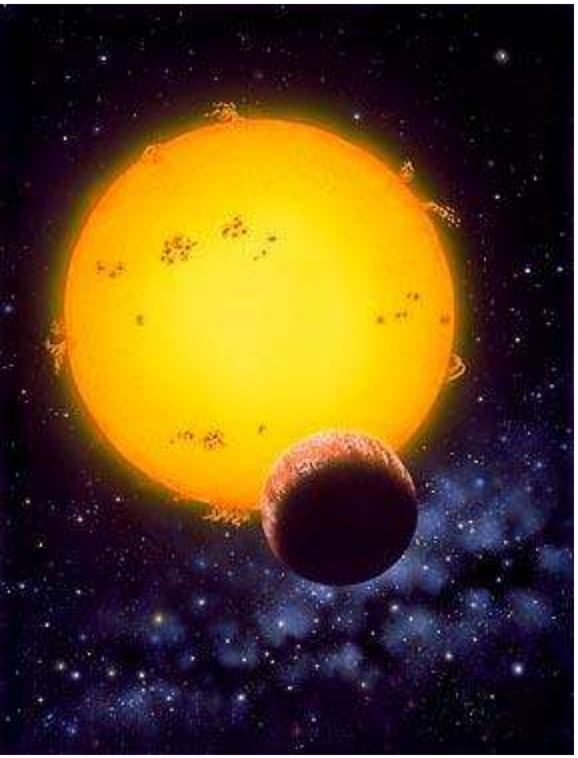

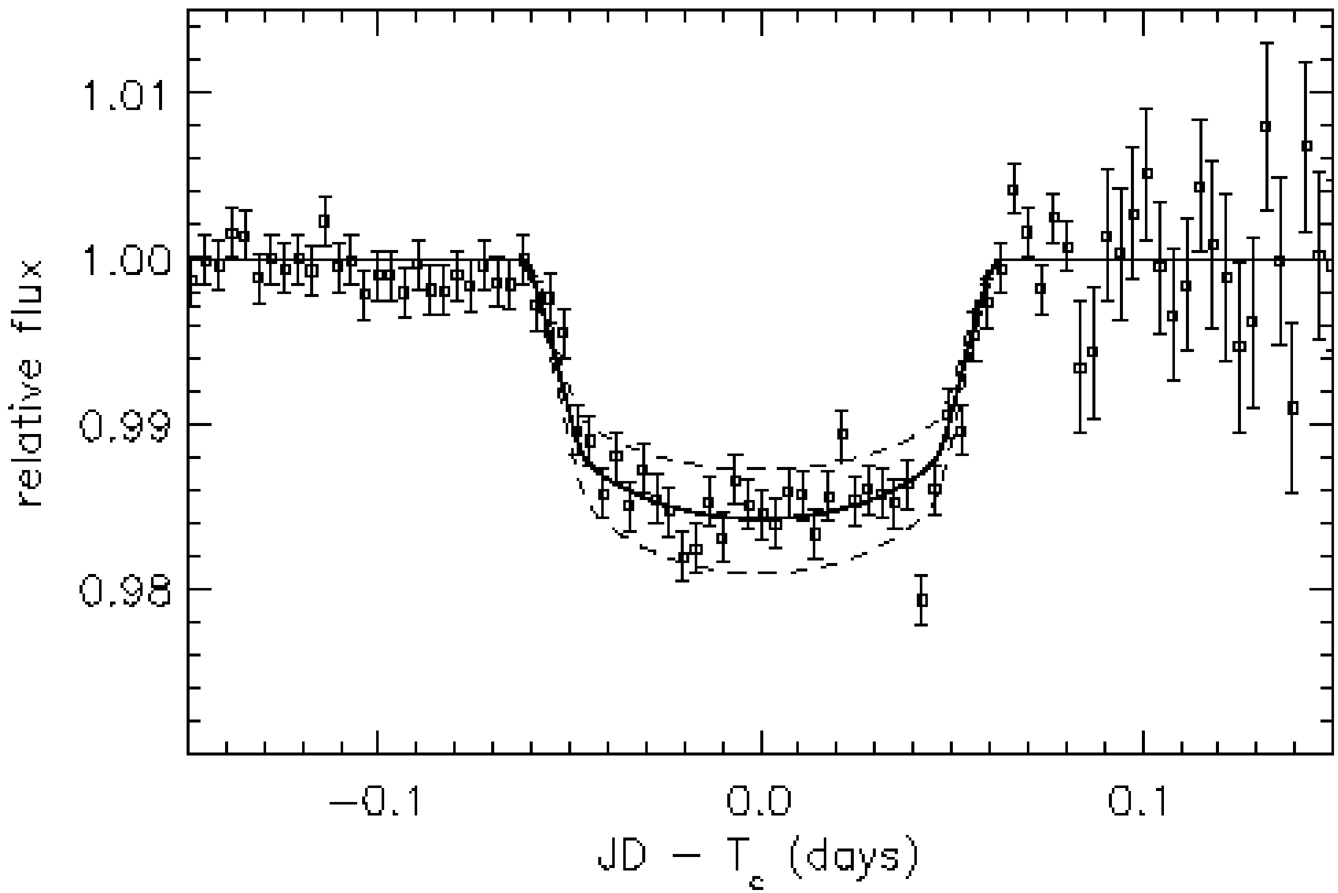

THE ASTROPHYSICAL JOURNAL, 529:L45–L48, 2000 January 20

DETECTION OF PLANETARY TRANSITS ACROSS A SUN-LIKE STAR

DAVID CHARBONNEAU,[1,2] TIMOTHY M. BROWN,[2] DAVID W. LATHAM,[1] AND MICHEL MAYOR[3]
Received 1999 November 19; accepted 1999 November 23; published 1999 December 16

Finding exoplanets: Transits

HD 209458

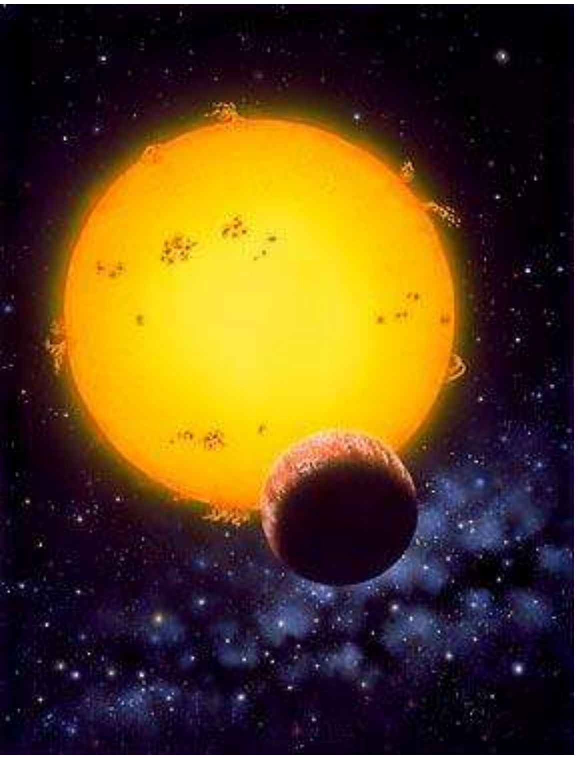

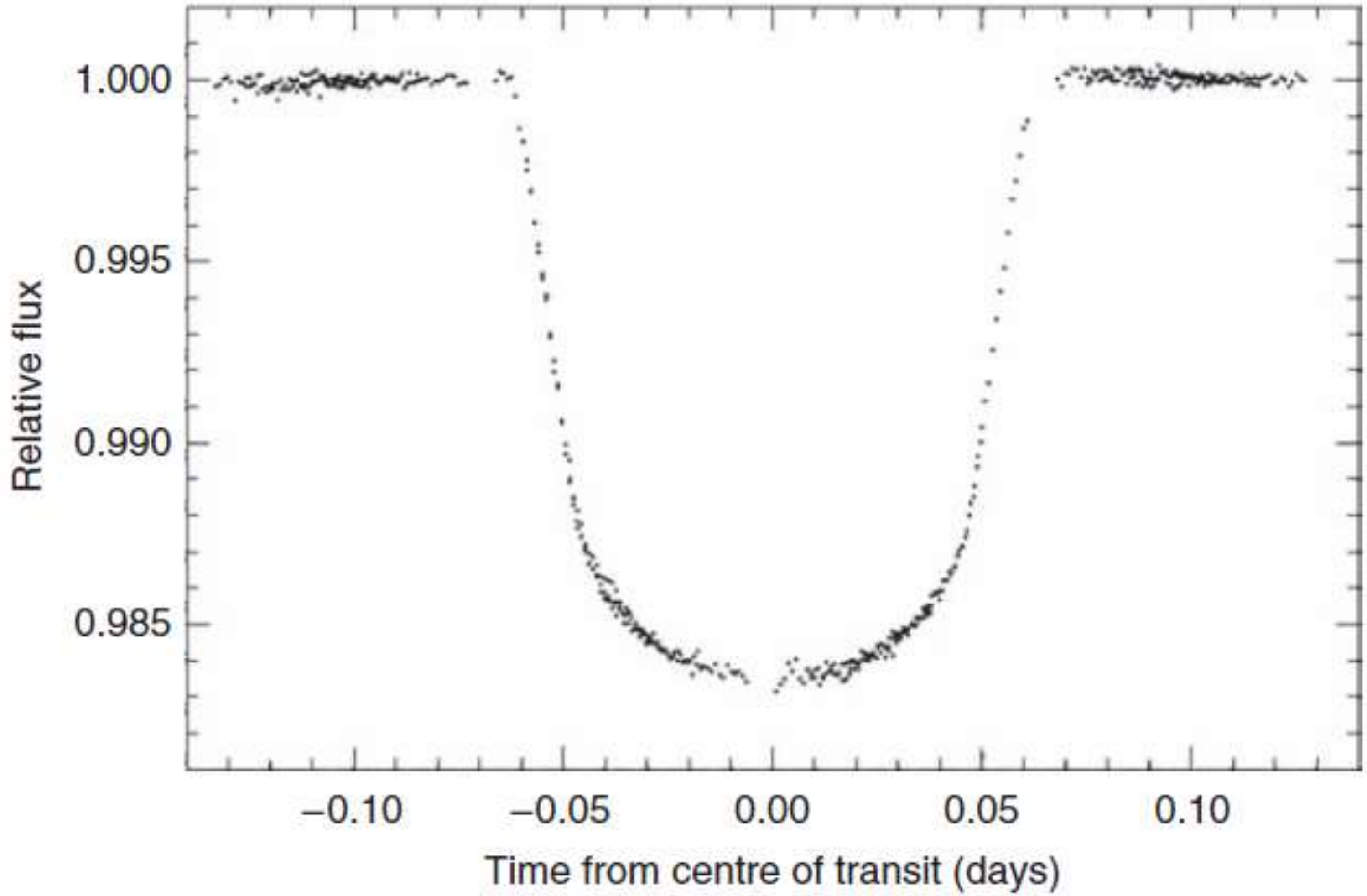

Figure 1.1 Eclipse of HD 209458 by its low-mass, presumed planetary, companion. The light curve has been combined from four separate recordings in April and May 2000 using the Imaging Spectrograph of the Hubble Space Telescope integrating over a yellow–orange region of the spectrum. Individual points are accurate to an estimated 1 part in 10 000. (From T. M. Brown *et al.*, 2001.)

Kepler

continuously and simultaneously monitors the brightnesses of more than 100,000 stars for the life of the mission—3.5 years

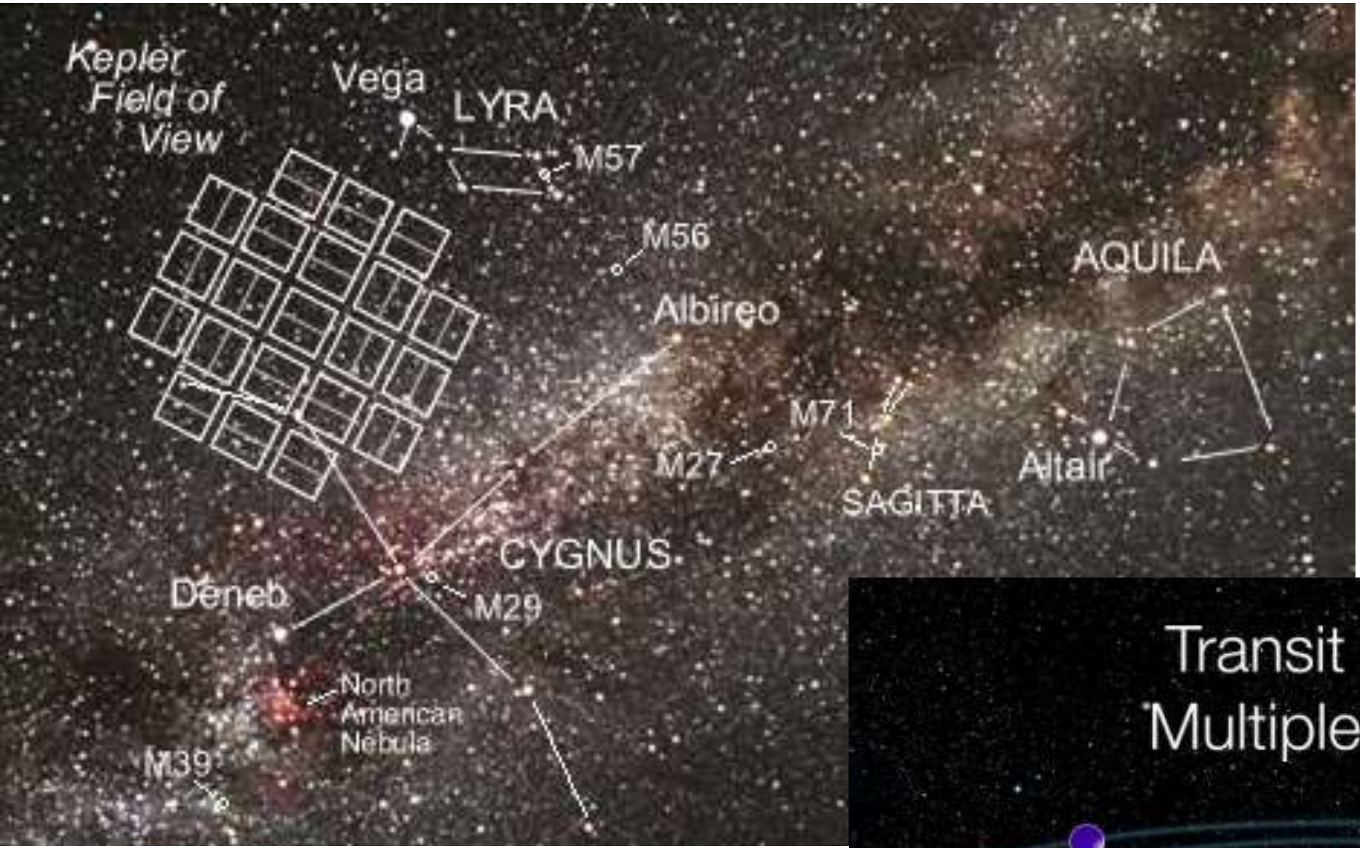

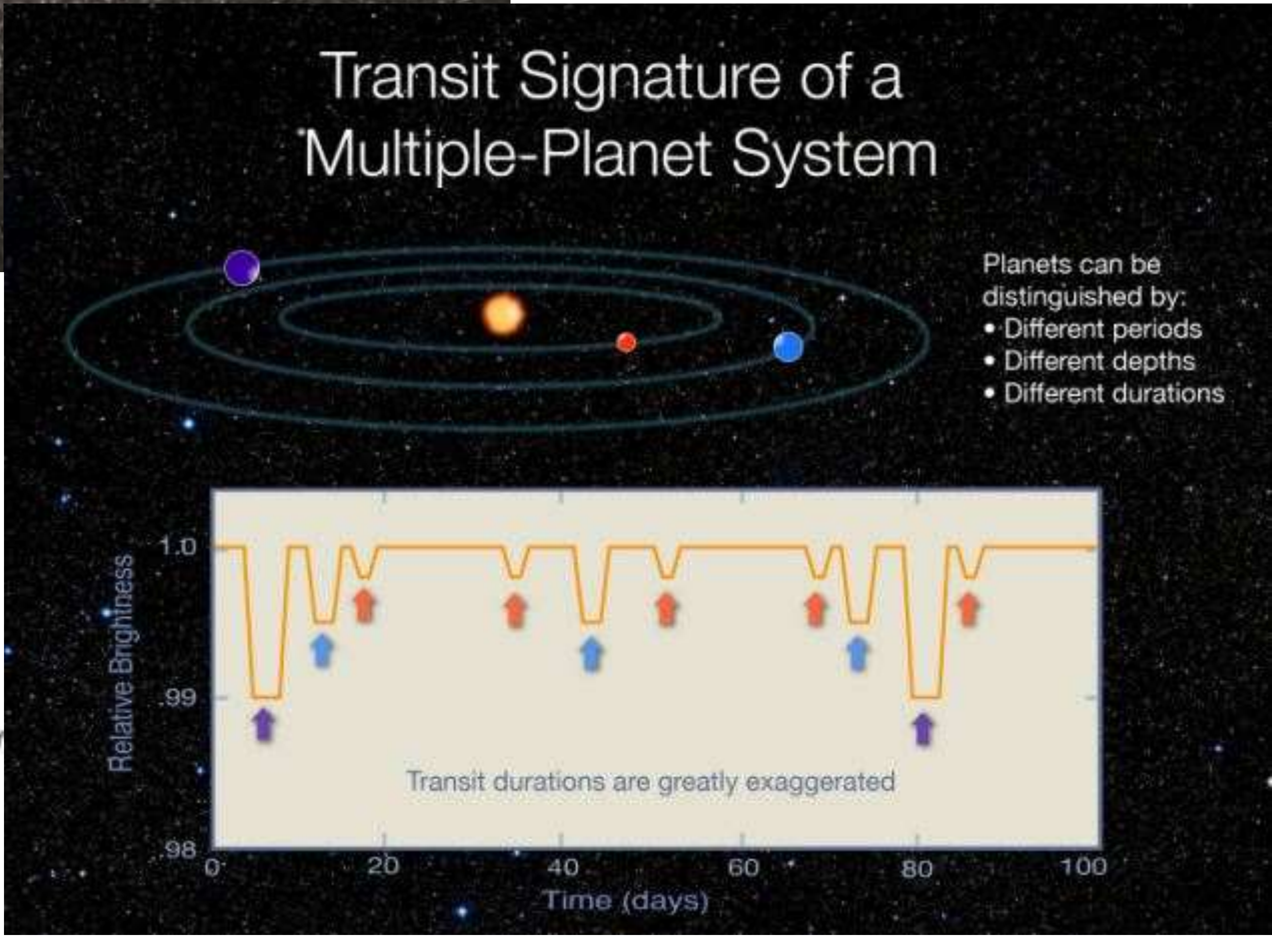

Filtros estreitos

Restritos a uma região espectral muito estreita (às veces apenas a uma linha), mas também é medido o continuo próximo

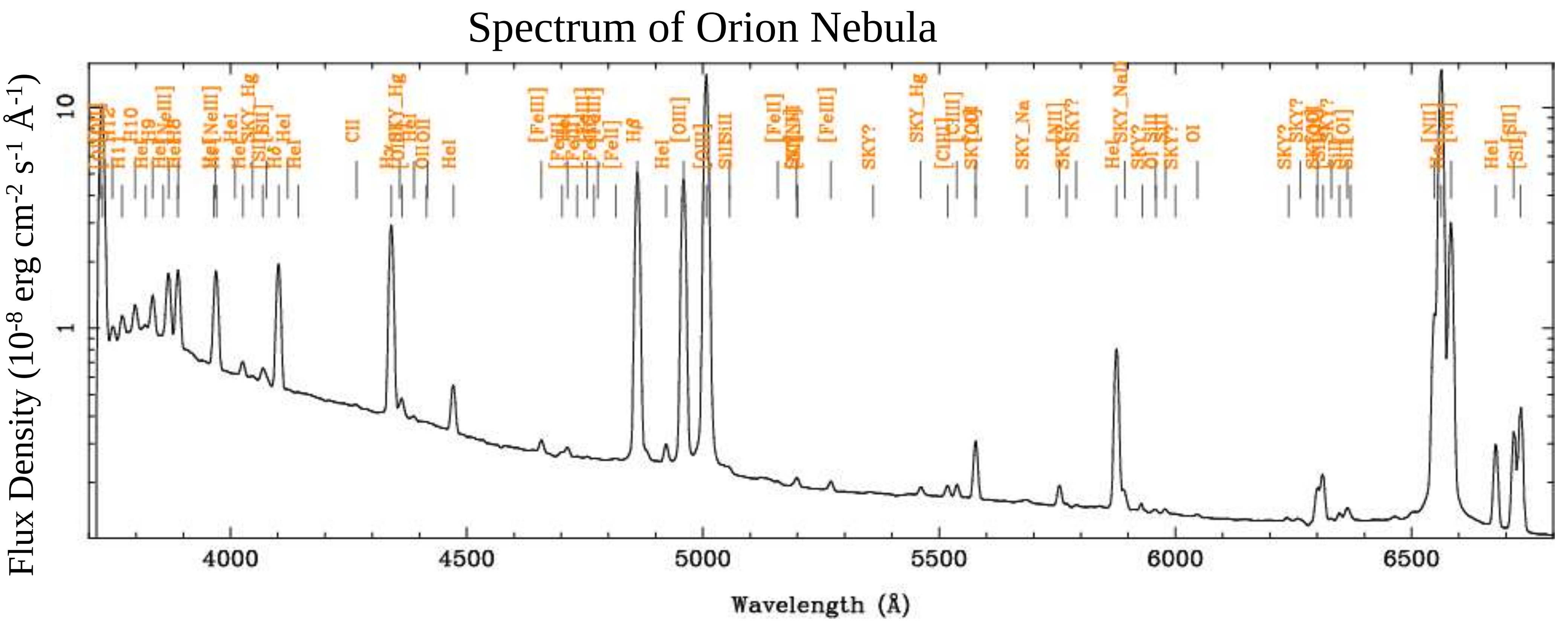

Exemplos

Nossa galáxia em um filtro largo (visível)

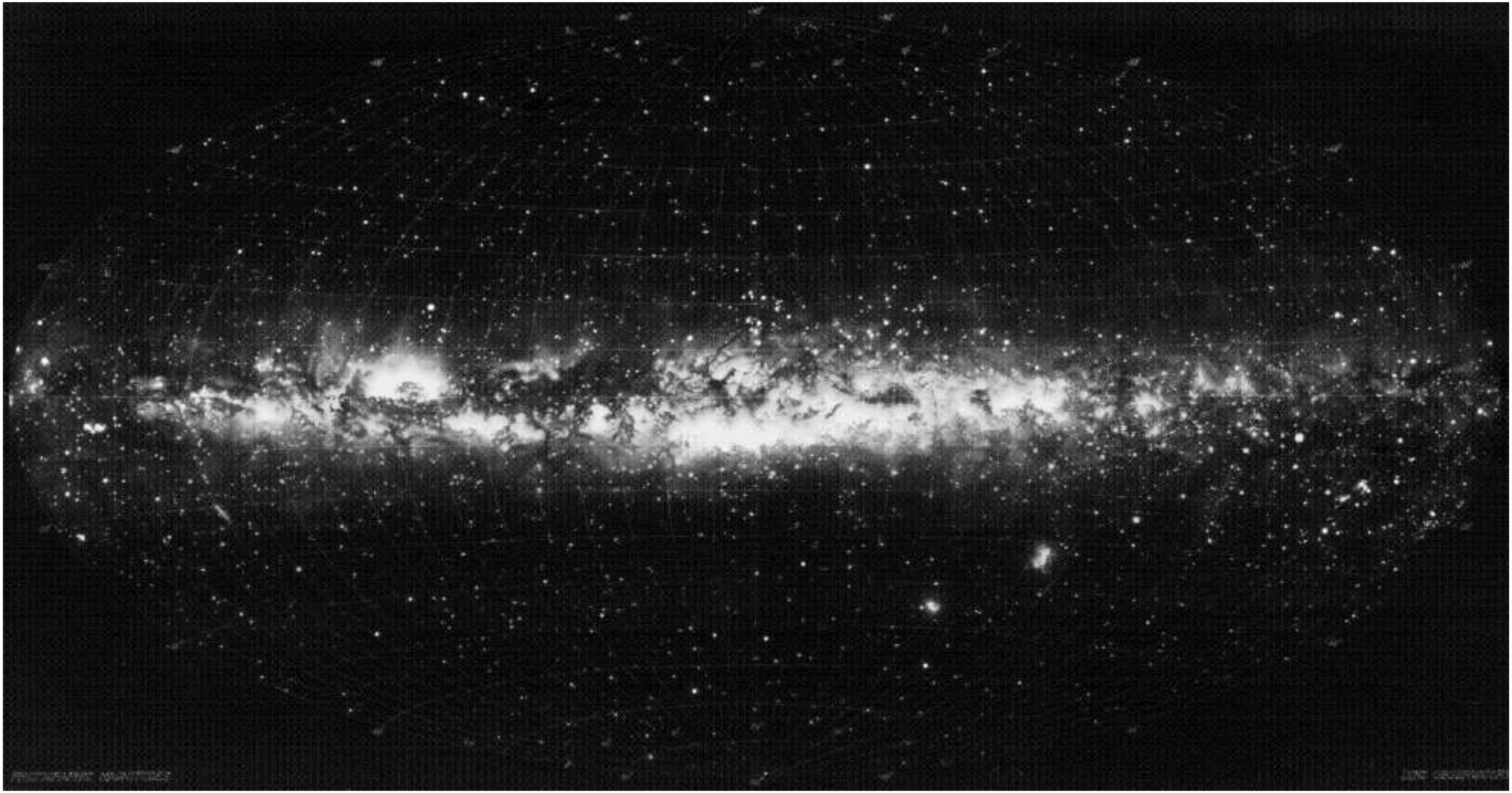

Exemplos

Nossa galáxia no filtro estreito de Hα

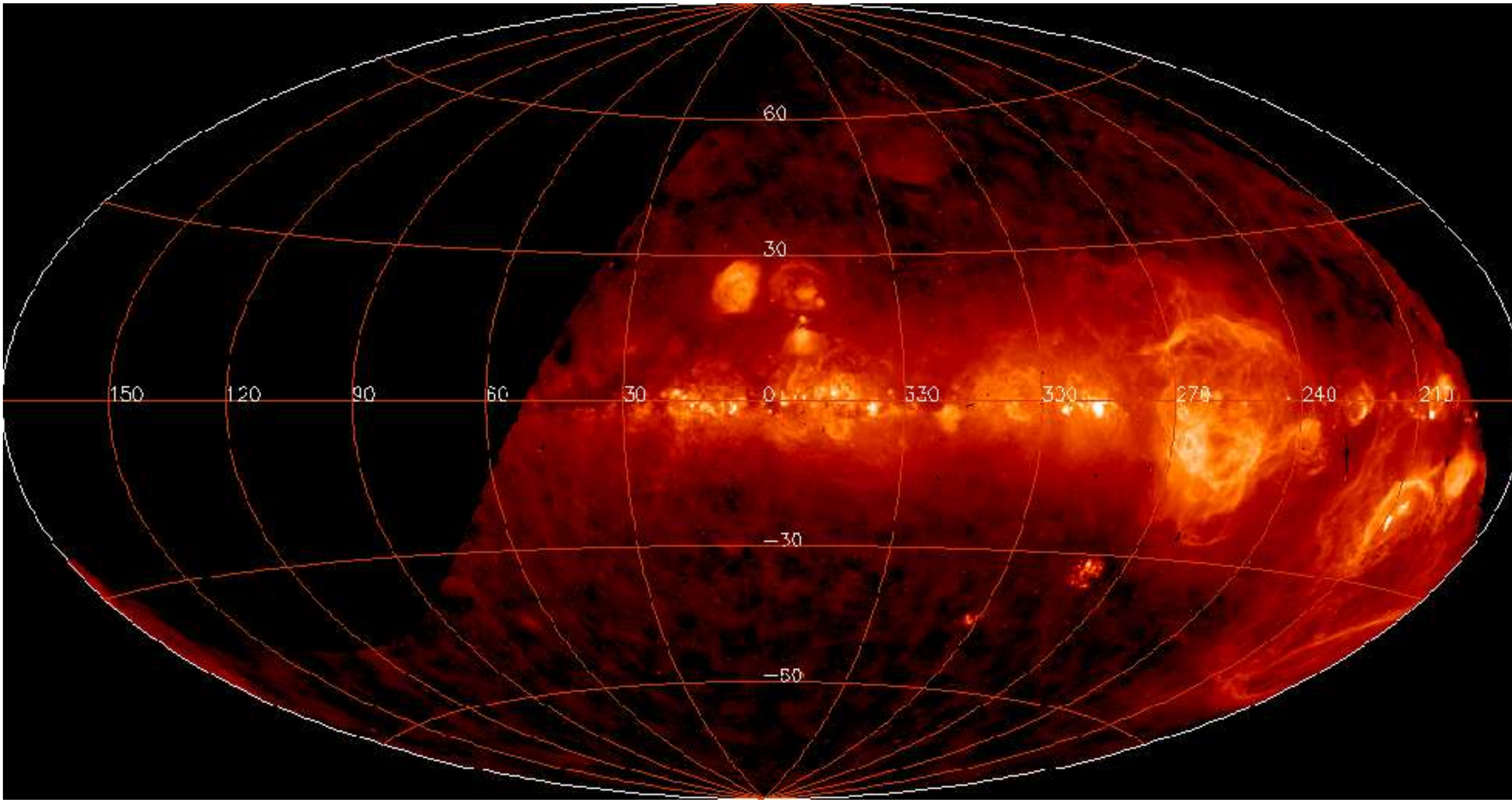

Exemplos

Andromeda em filtro estreitos de Hα e contínuo

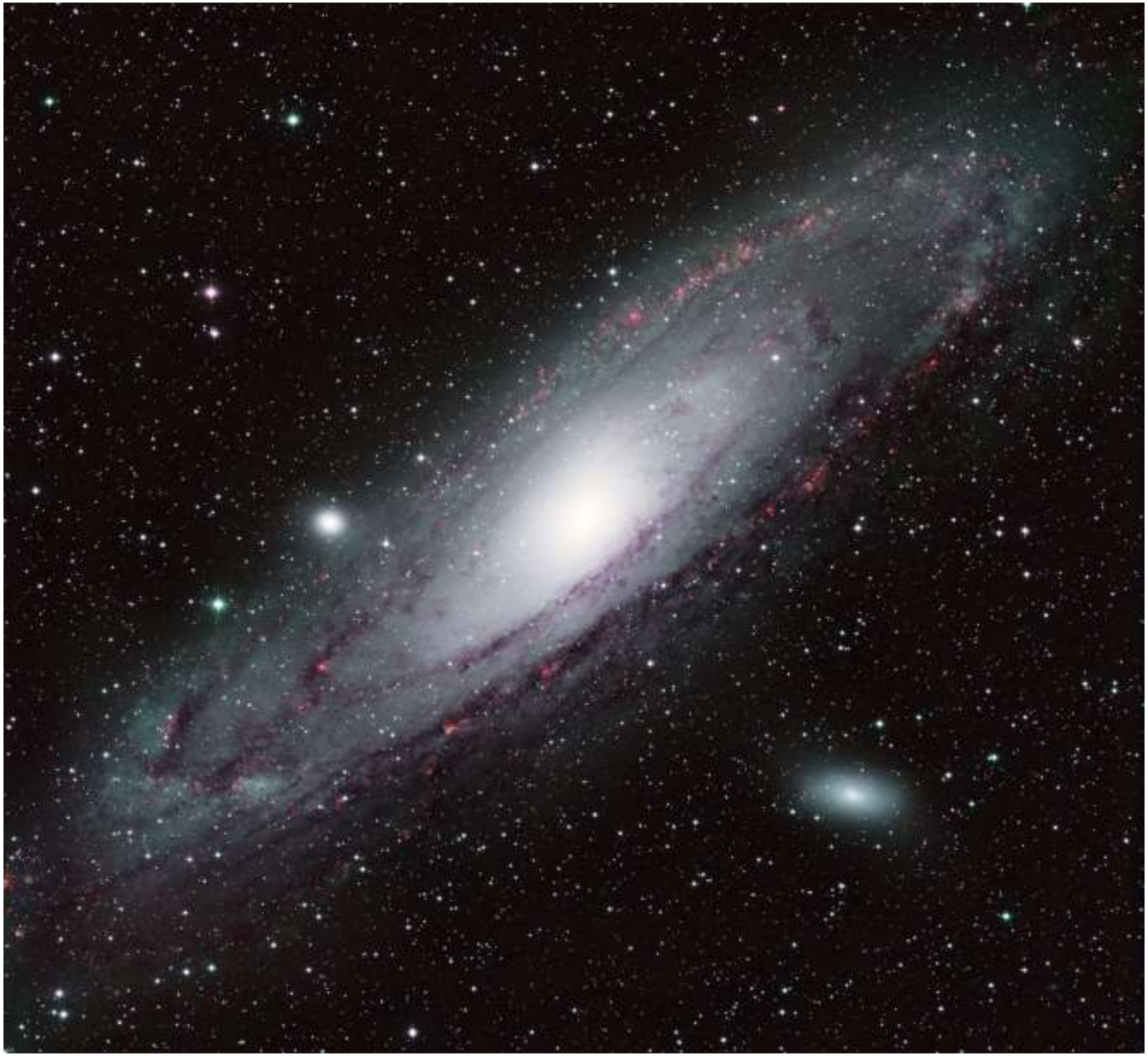

Exemplos

Andromeda em filtro de Hα (contínuo subtraido)

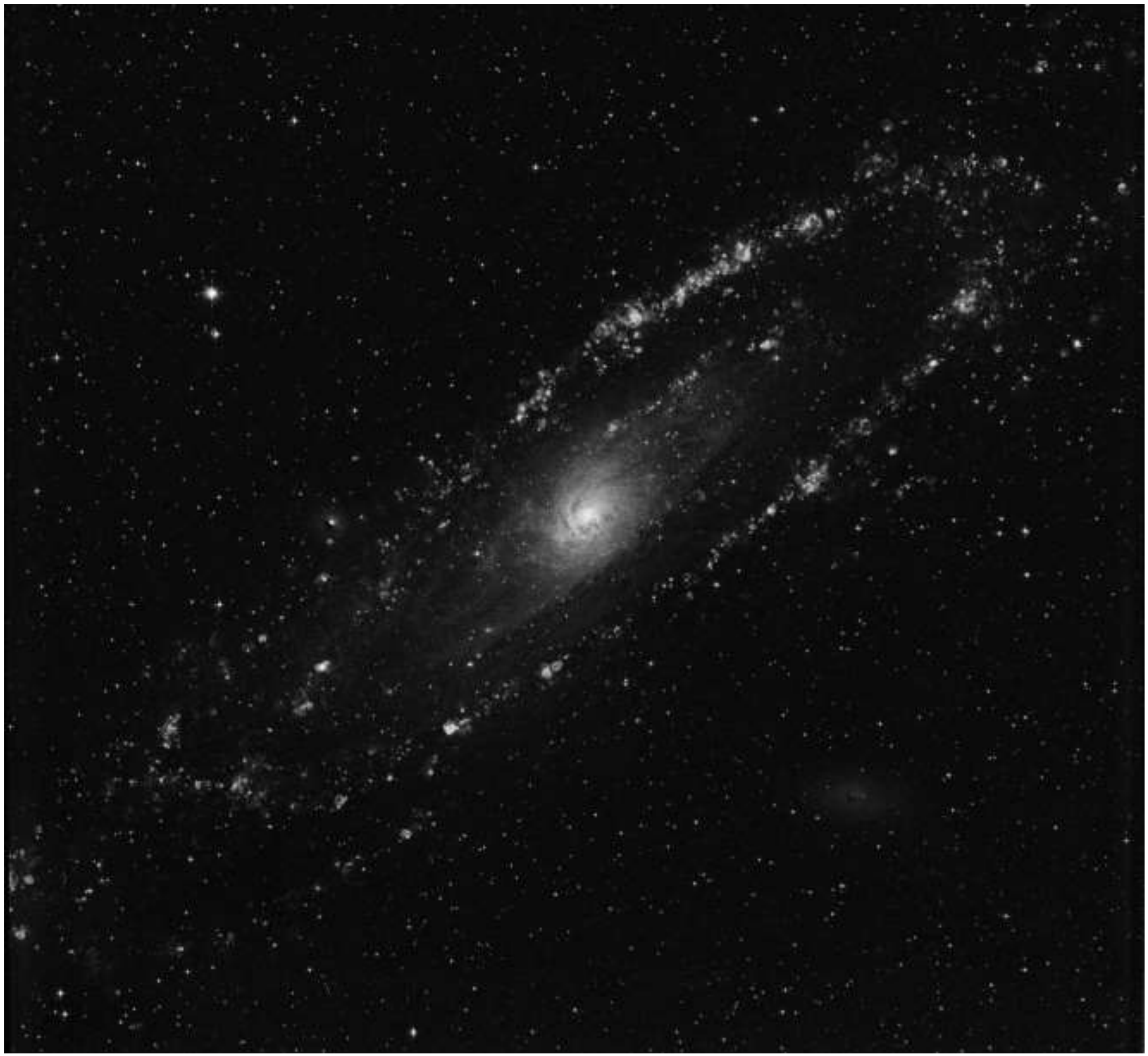

Missão no OPD

- 1 abril 2014, 15:45

atendendo sua solicitação, concedemos as noites de 12 e 13 de abril nos telescópios P&E e B&C, para treinamento de alunos do IAG/USP, projeto este que receberá a denominação LNA2014A/P-044. O telescópio P&E estará equipado com o ECass 600 e o B&C com a Cam+Ikon.